

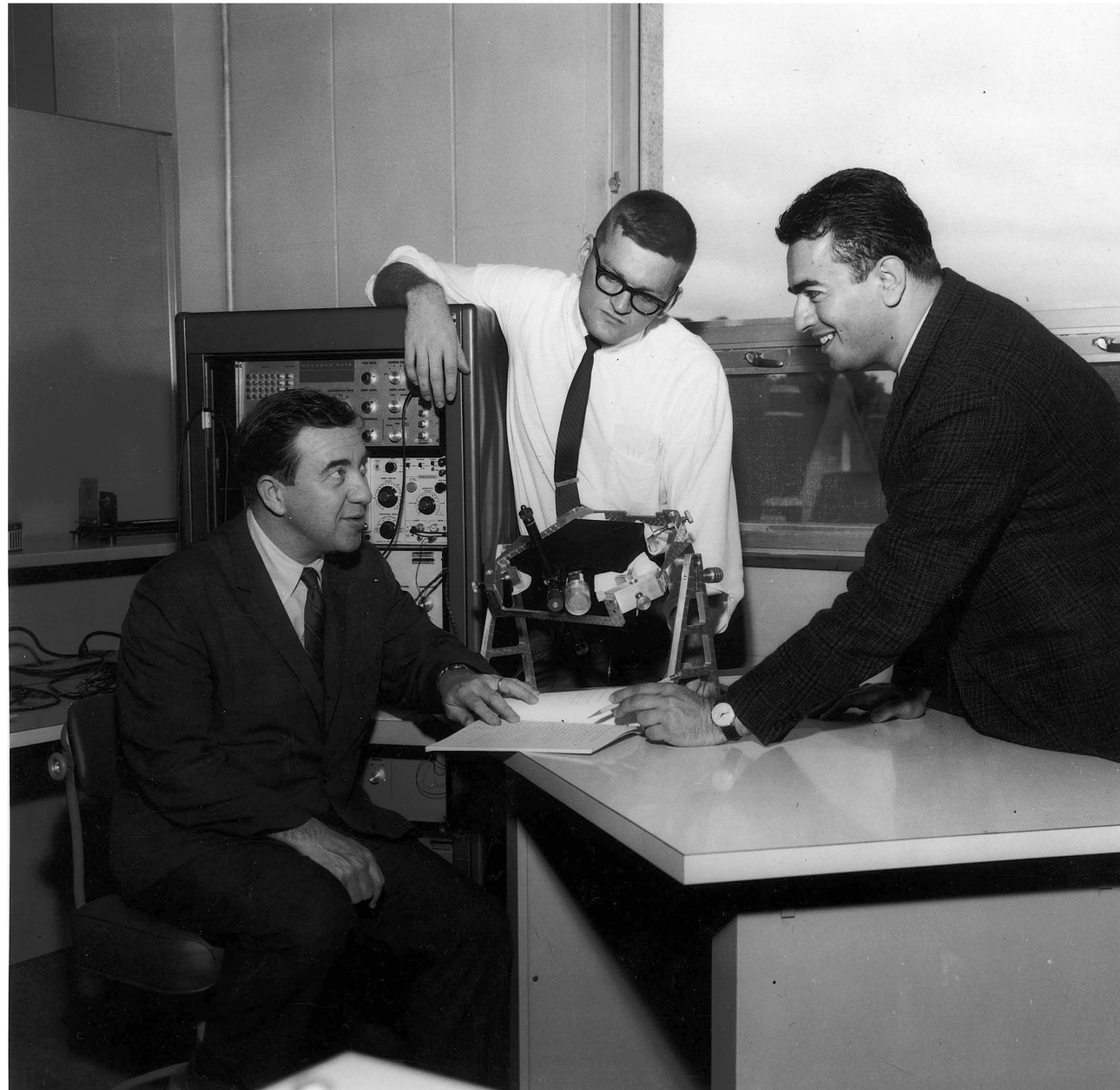
Planetary Magnetospheres: Van Allen Belts of Solar System Planets

Stamatios M. Krimigis

Applied Physics Laboratory, Johns Hopkins University,
Laurel, MD, 20723

*Van Allen Day Symposium
Van Allen Hall
University of Iowa, Iowa City, IA
9 October, 2004*

J. A. Van Allen, T. P. Armstrong, and S. M. Krimigis at U of I, 1966



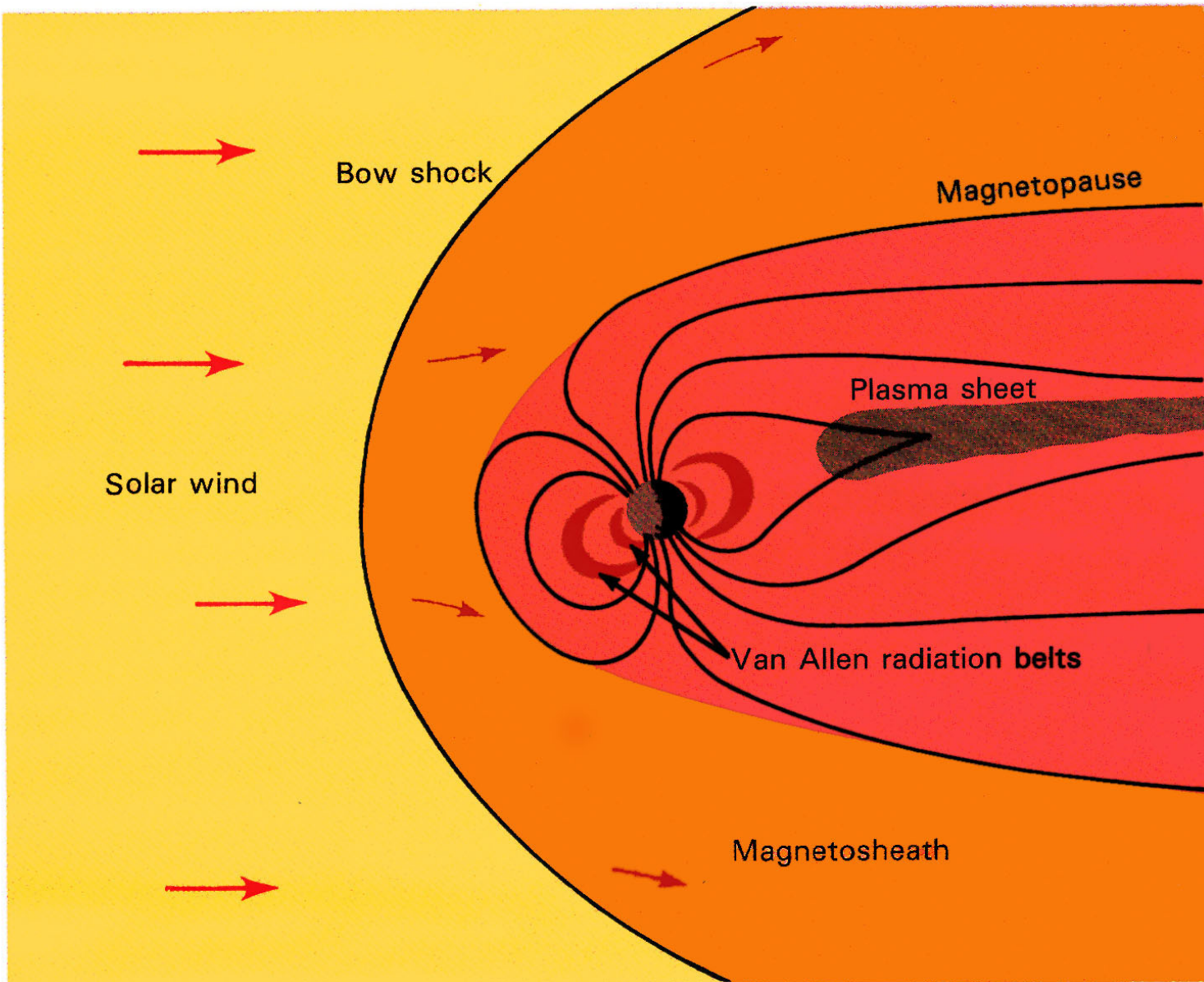
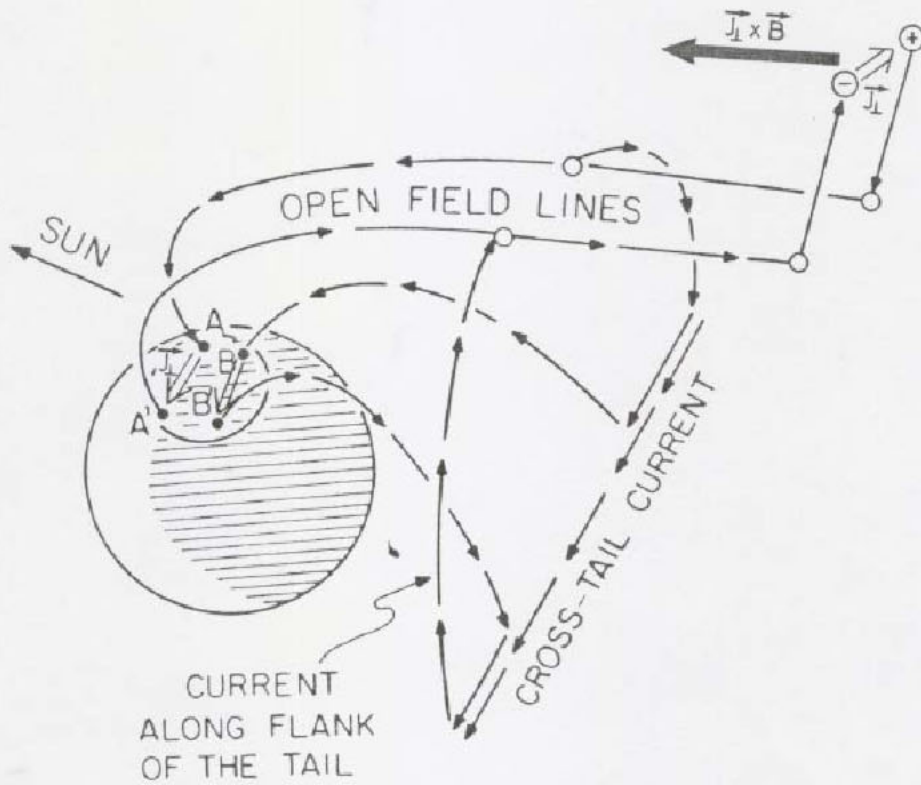


Figure 1—Earth's magnetosphere. The sketch shows important features of the plasmas and waves in the magnetic fields that surround Earth.

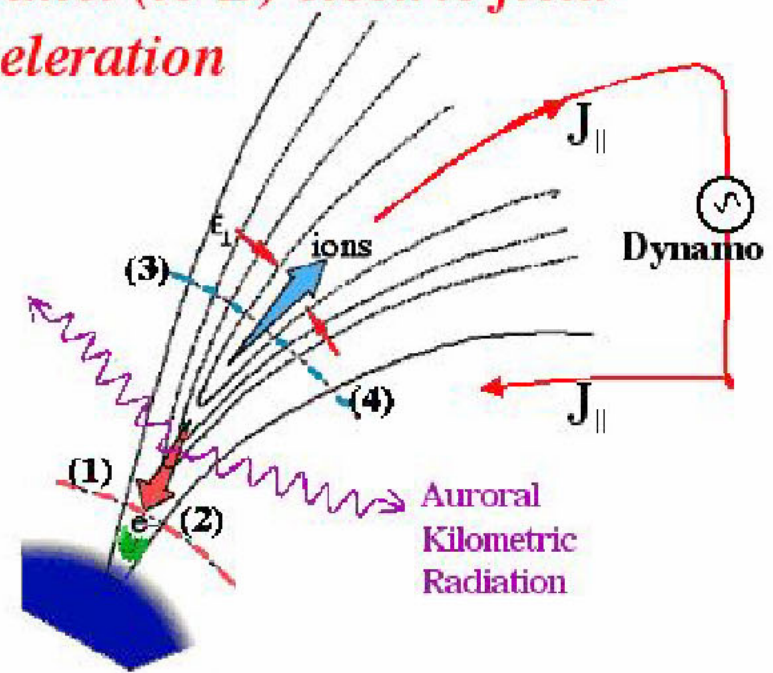
Lanzerotti, L. J. and S. M. Krimigis, Comparative magnetospheres, *JHU/APL Tech. Dig.*, 7, 335-347, 1986.



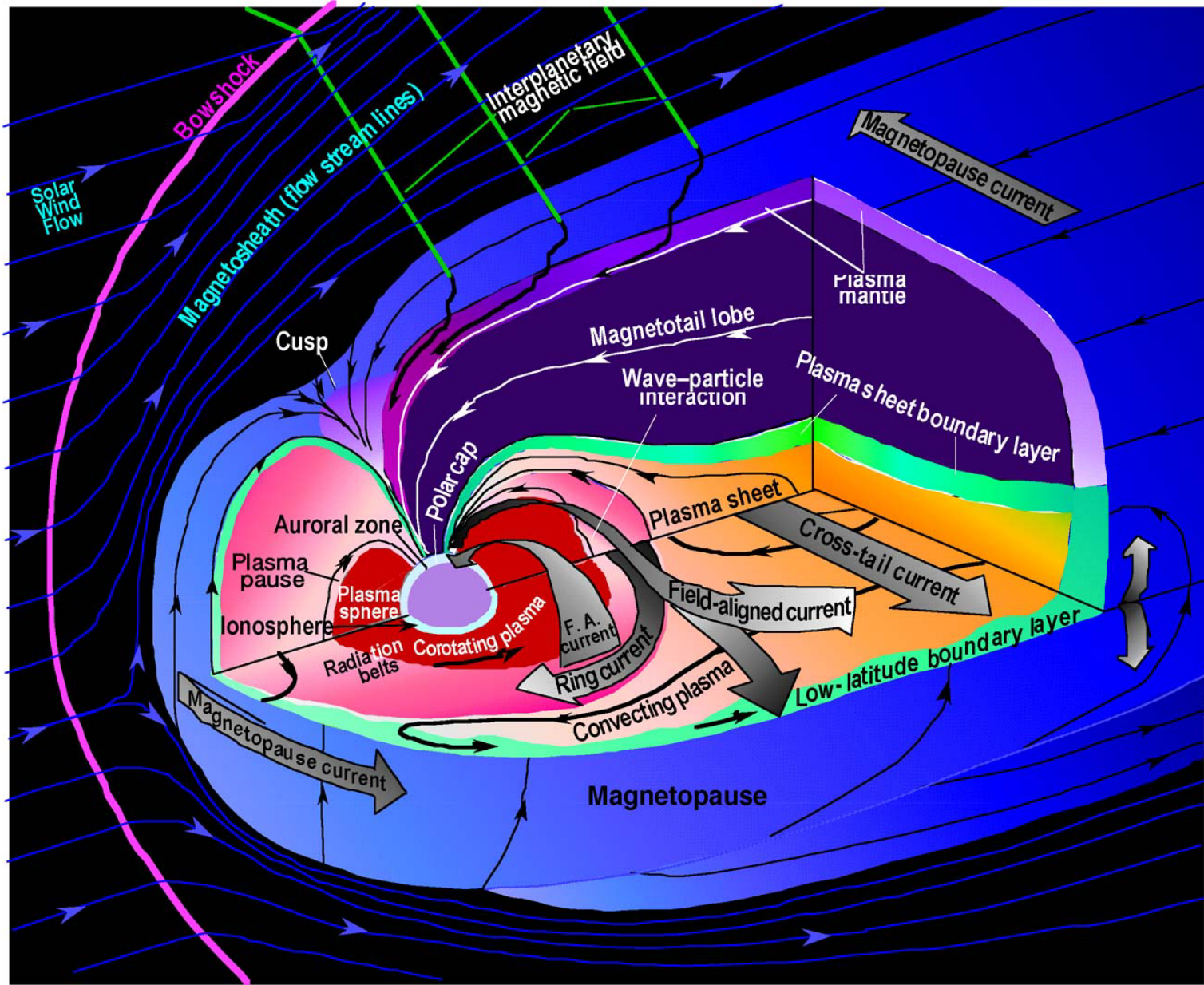
Auroral currents :

A great example of
multiscale physics

*Parallel (to B) electric field
acceleration*



Earth's Magnetosphere



ACT 3 :
SOLAR SYSTEM
MAGNETOSPHERES
(Blanc, 2004)

LISM



HELIOSPHERE



« INTRINSIC »

MAGNETOSPHERES

Giant Planets

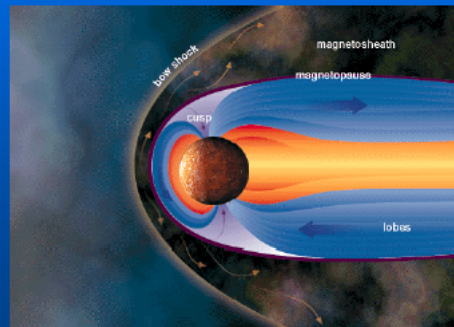


Satellite Magnetospheres



Intrinsic

Earth,
Mercury



Induced

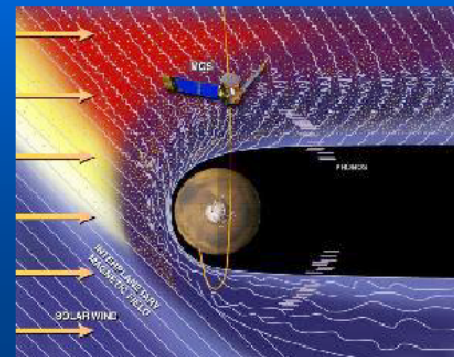
Titan



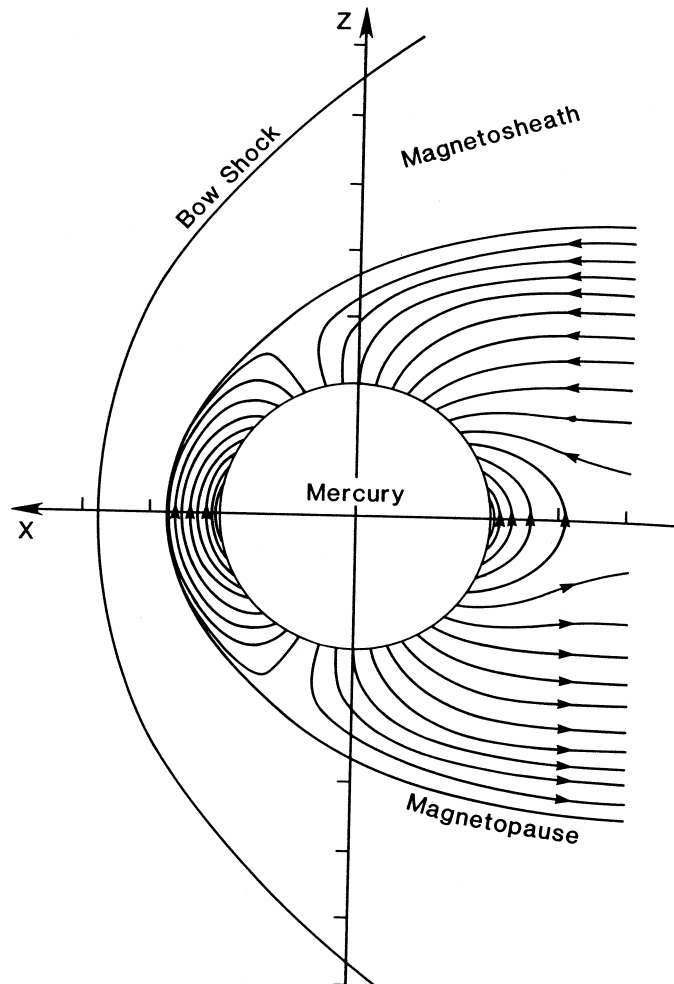
Induced magnetospheres

Venus, comets

Mars ?



Mercury's Magnetic Field



- Not even dipole term well-resolved by Mariner 10 data.
- Competing hypotheses for the internal field (remanence, hydromagnetic dynamo, thermoelectric currents) predict different field geometries.
- Internal field can be separated from external field by repeated orbital measurements.
- Mercury's magnetosphere provides an important comparison to that of Earth.

Mercury's magnetosphere [Russell et al., 1988].

Plasma and Energetic Particles- Magnetospheric Boundary Layer (Christon, JGR 94, 6481, 1989)

CHRISTON: ELECTRONS AT MERCURY'S MAGNETOSPHERIC BOUNDARY LAYER

6483

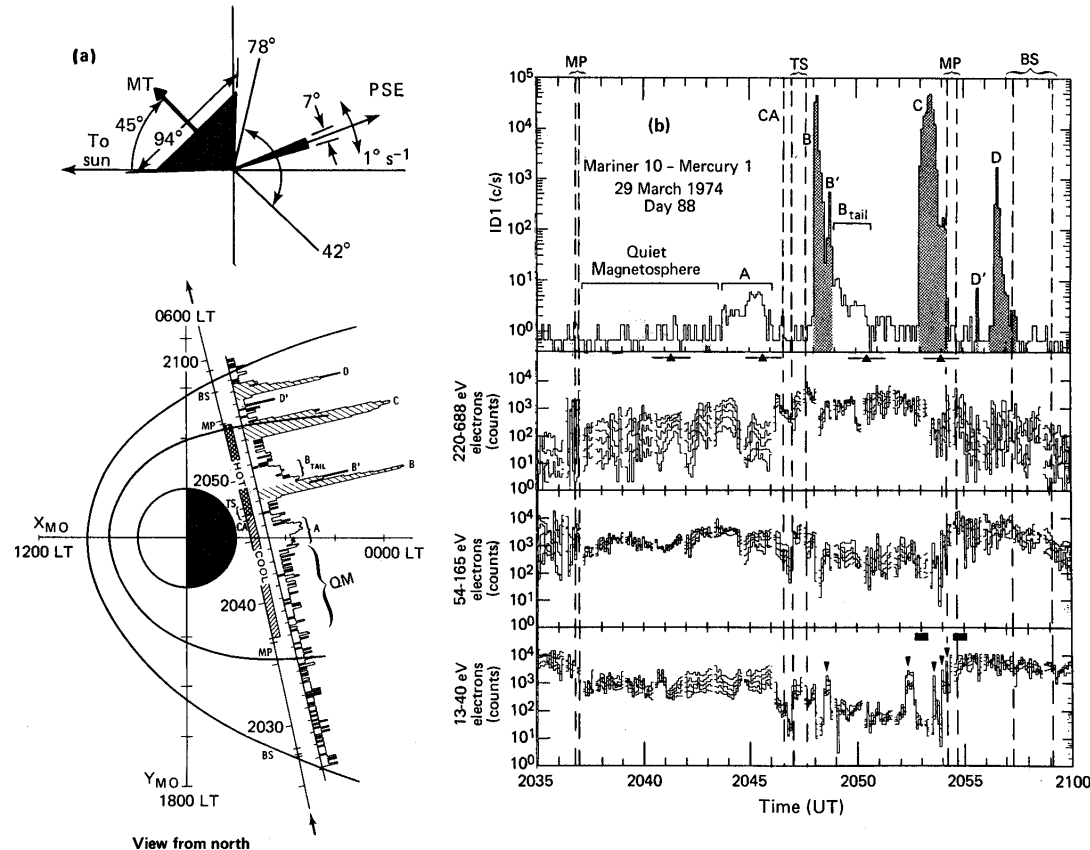


Fig. 1. (a) The X_{MO} - Y_{MO} projection of Mariner 10's trajectory at Mercury 1 on day 88, 1974 (indicated by arrows) is shown in Mercury Orbital MO coordinates (described in the text). Cool and hot plasma regions as well as principal analysis periods are indicated. The (un)shaded portion of the 6-s average ID1 counting rate of the main telescope (MT), which is offset from the trajectory, identifies (>175) >35 keV electron fluxes. Local times are shown. Insert at top shows view directions and angular openings of the MT and PSE electron analyzer (see Eraker and Simpson [1986] and Ogilvie et al. [1977], respectively, for details). (b) Simultaneous 6-s averages of >35 keV or >175 keV ID1 electron data are compared to 13.4-688 eV plasma electron data (6-s samples of 15 logarithmic, equally spaced, energy channels of the PSE electron analyzer are separated into three groups of five adjacent channels). The (un)shaded portion of the ID1 counting rate identifies (>175) >35 keV electron fluxes. Highlighted periods are discussed in text.

Reinterpretation of Energetic Particle Fluxes at Mercury (Armstrong, Krimigis, Lanzerotti, JGR, 80, 4015, 1975)

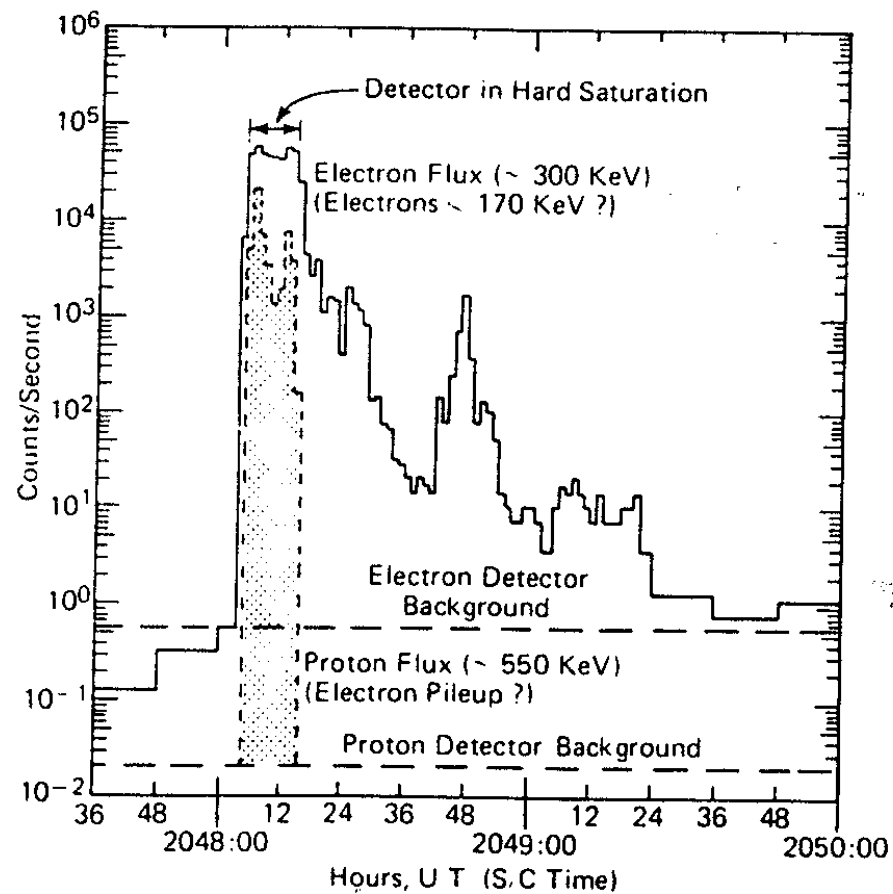
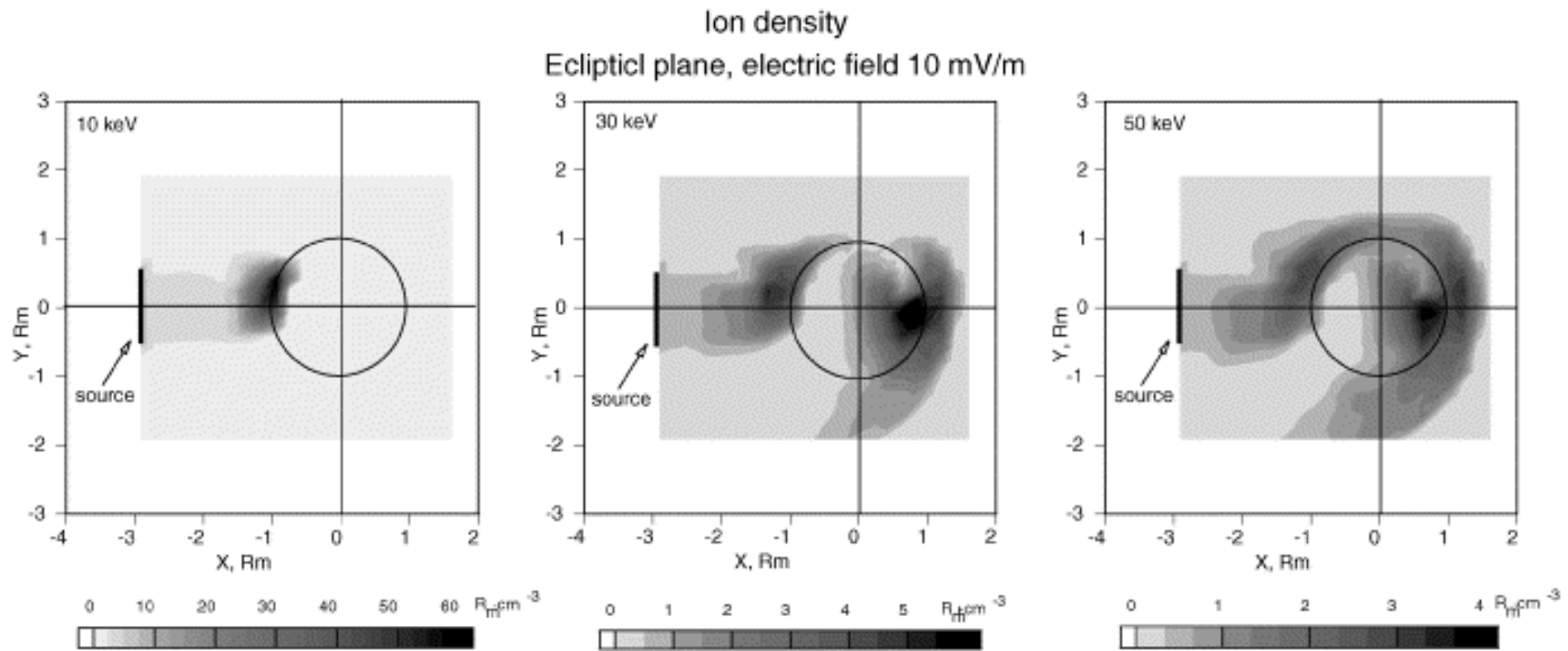


Fig. 1. The B event during Mercury encounter, adapted from *Simpson et al.* [1974a]. The labels 'electron flux (~ 300 keV)' and 'proton flux (~ 550 keV)' are those of *Simpson et al.* [1974a]. All other labels have been added, with the exception of the label on the time axis.

The column density of protons injected from the source with the central energy 10, 30, and 50 keV in the ecliptic plane. The convection electric field is 10 mV/m. The parallel component was assumed to be zero ([Lukyanov et al, Planet. Space Sci., 49, 1677, 2001](#)).



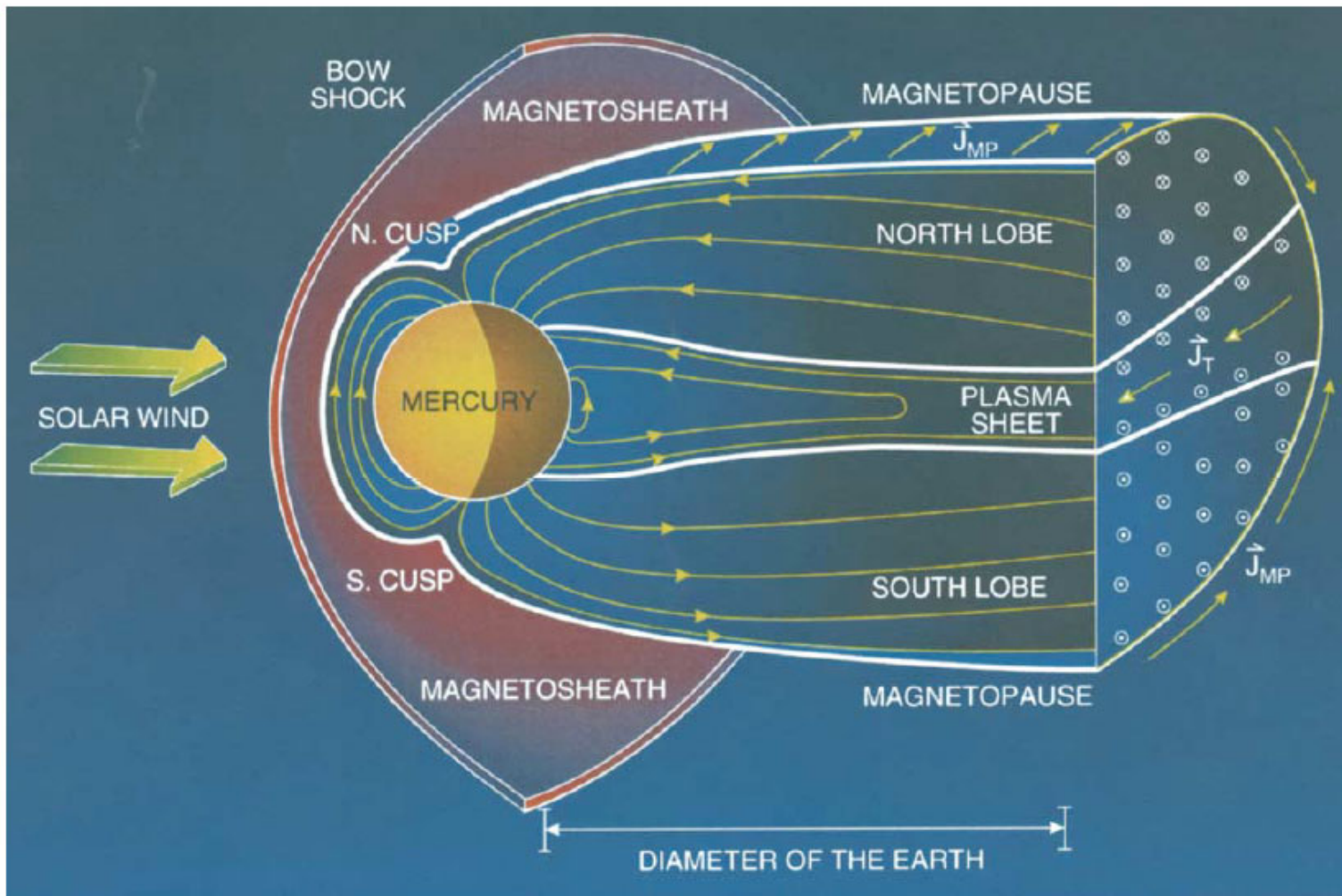
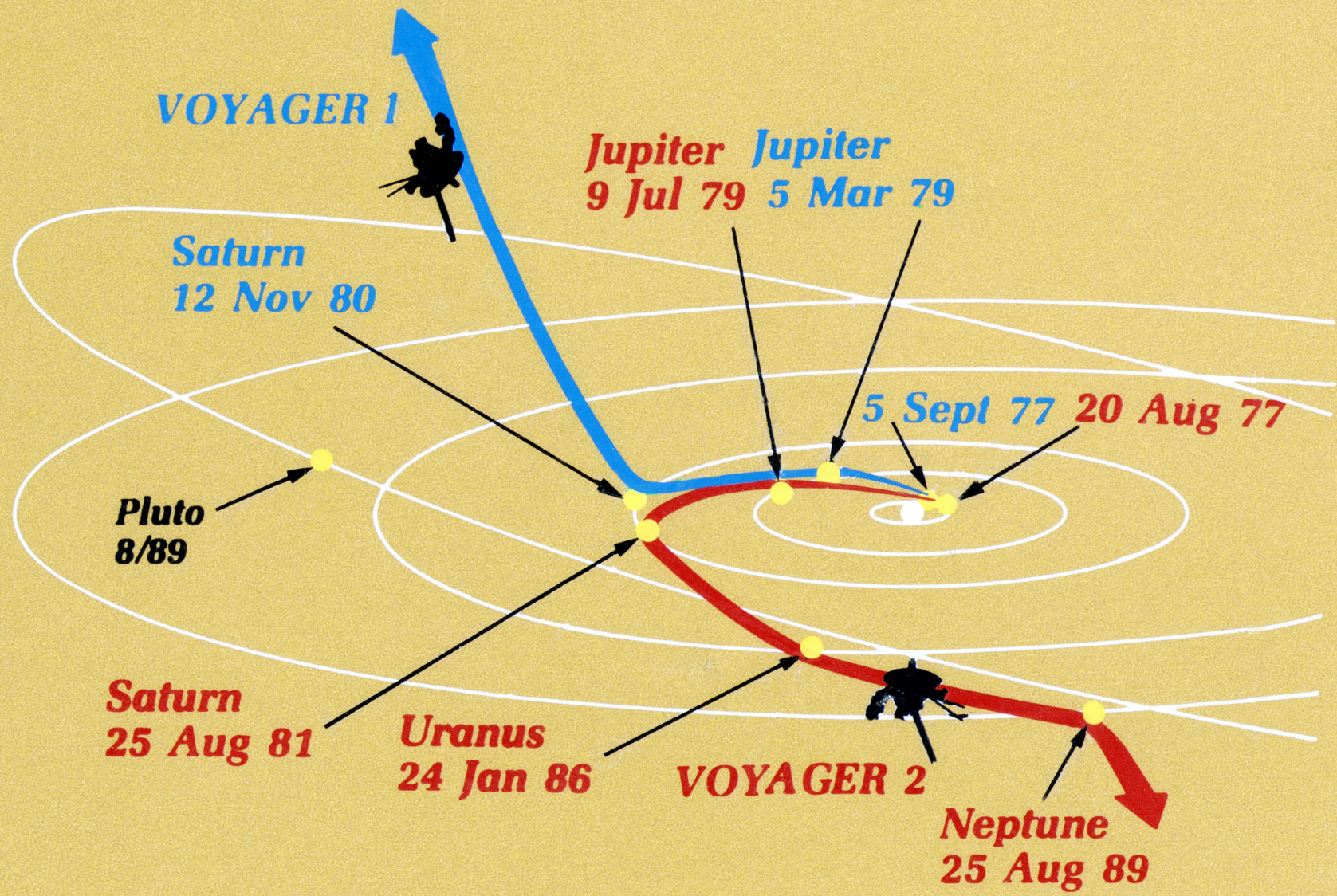


Fig. 2. Schematic view of the bow shock and magnetosphere of Mercury.

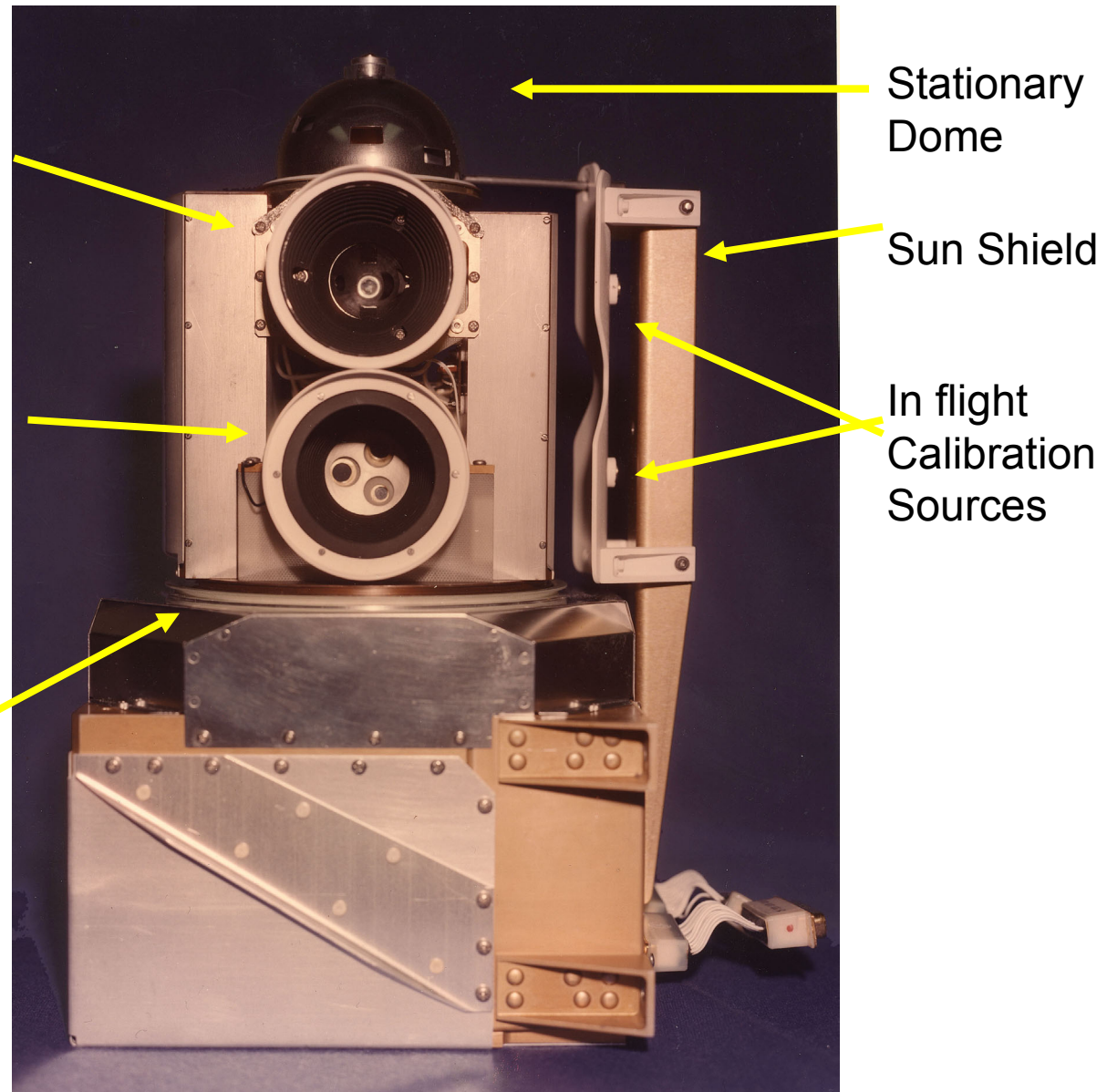


Low Energy Charged Particle Instrument on Voyager

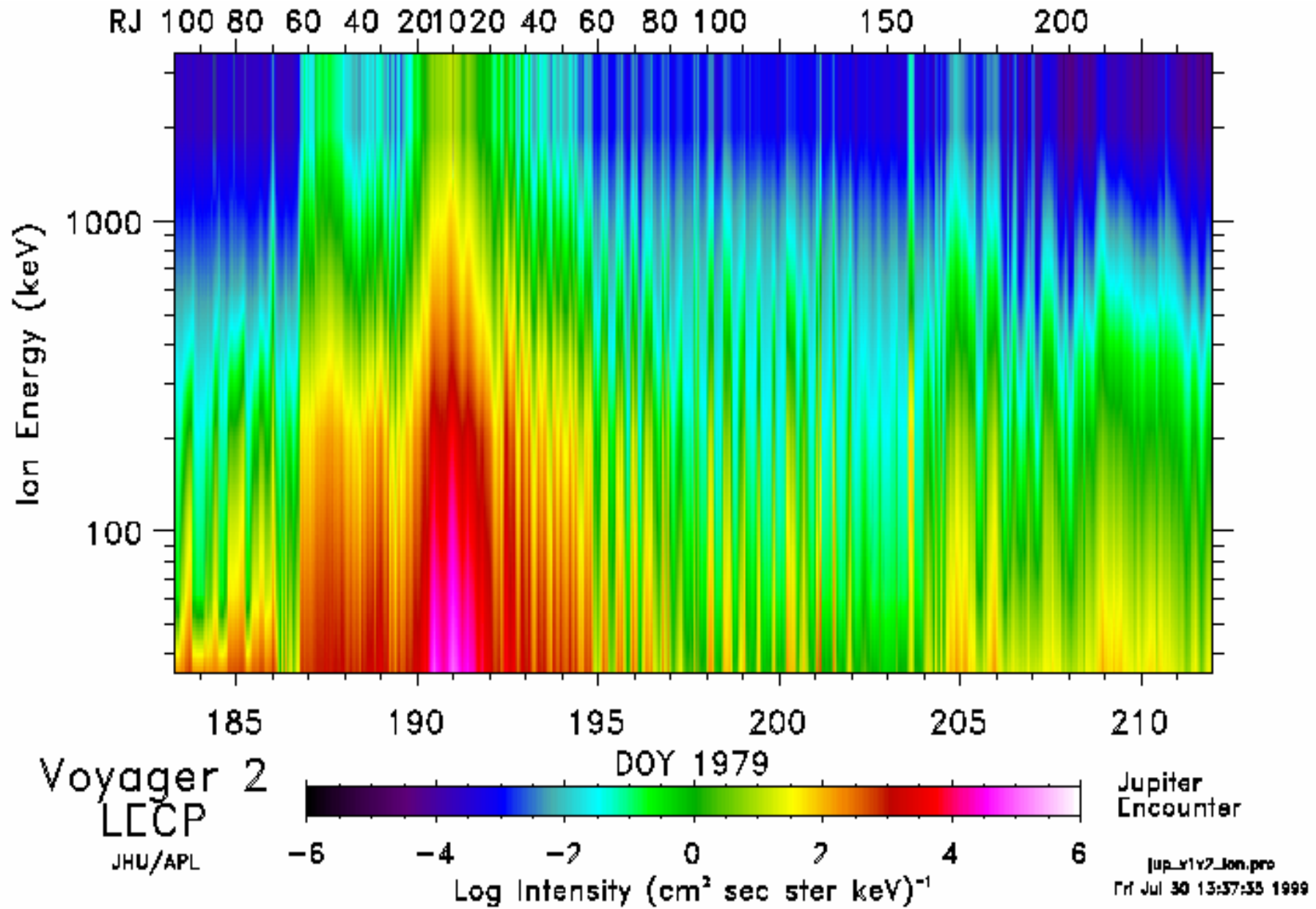
Low Energy
Magnetospheric
Particle
Analyzer

Low Energy
Particle
Telescope

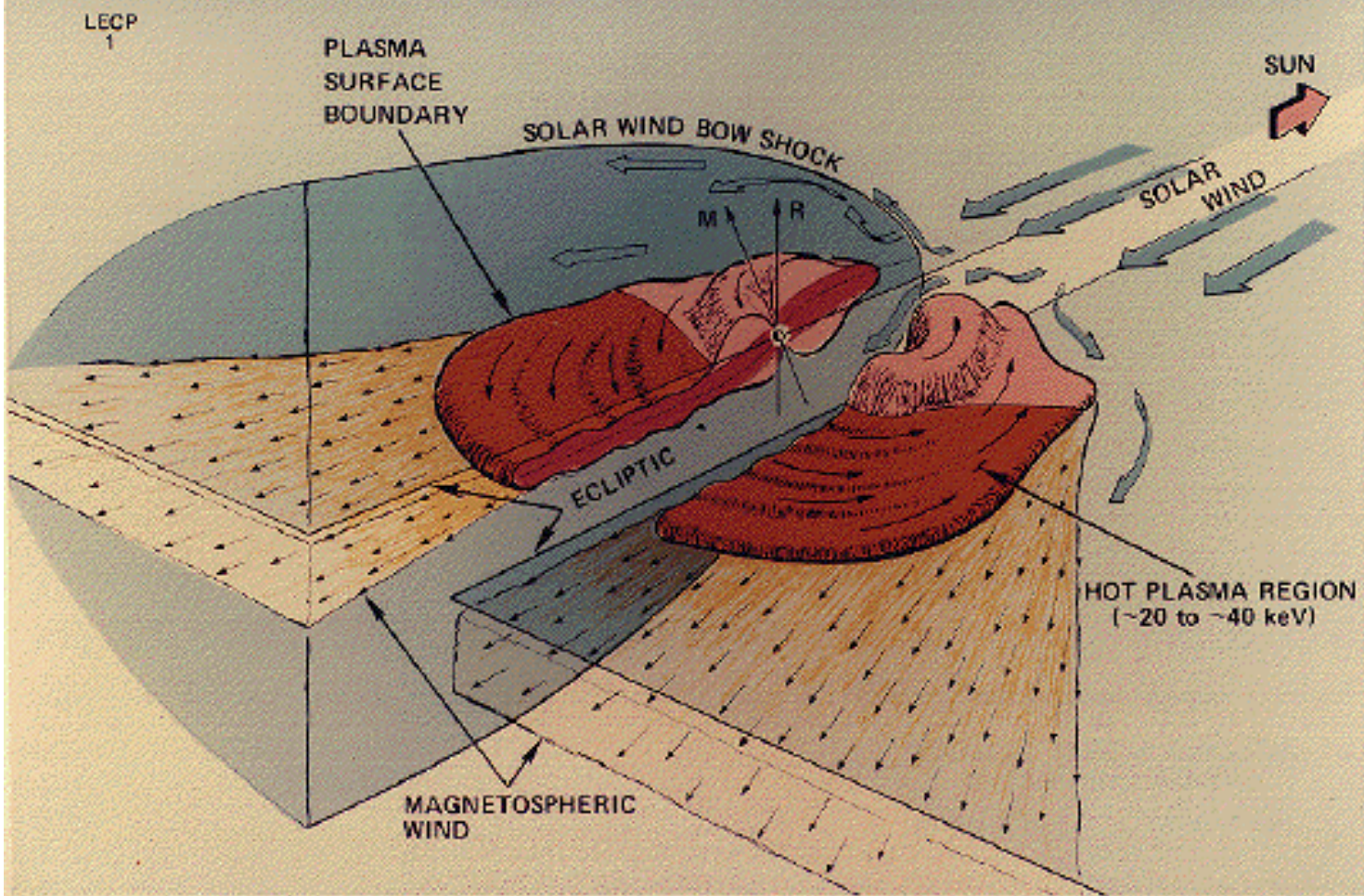
Rotating
Stepper
Platform



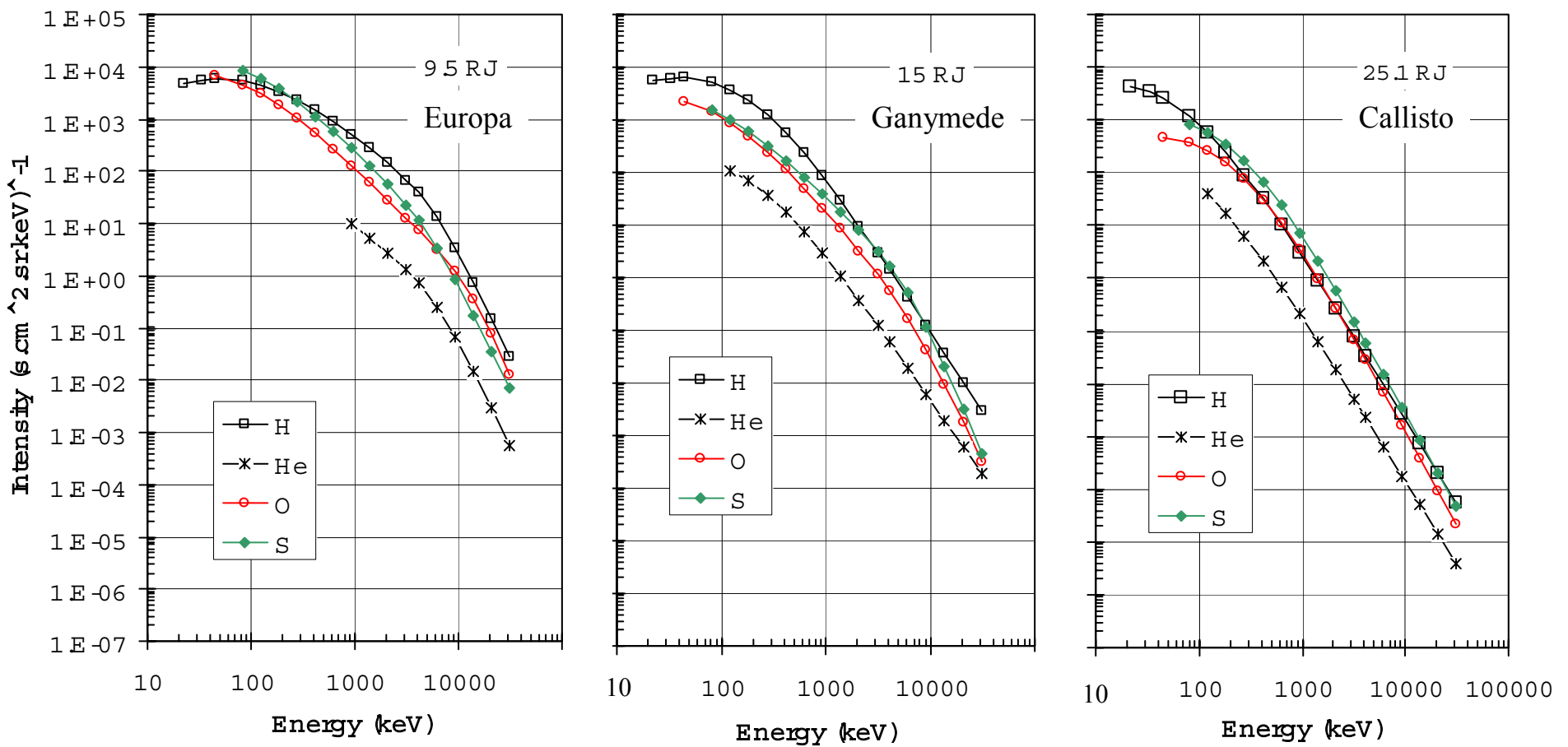
Ion Intensities in Jupiter's Magnetosphere, Voyager 2, 1979



JUPITER'S MAGNETOSPHERE



The “typical” intermediate-energy energetic ion spectra near the icy moons are well characterized by Galileo.



Krupp et
al., 2001

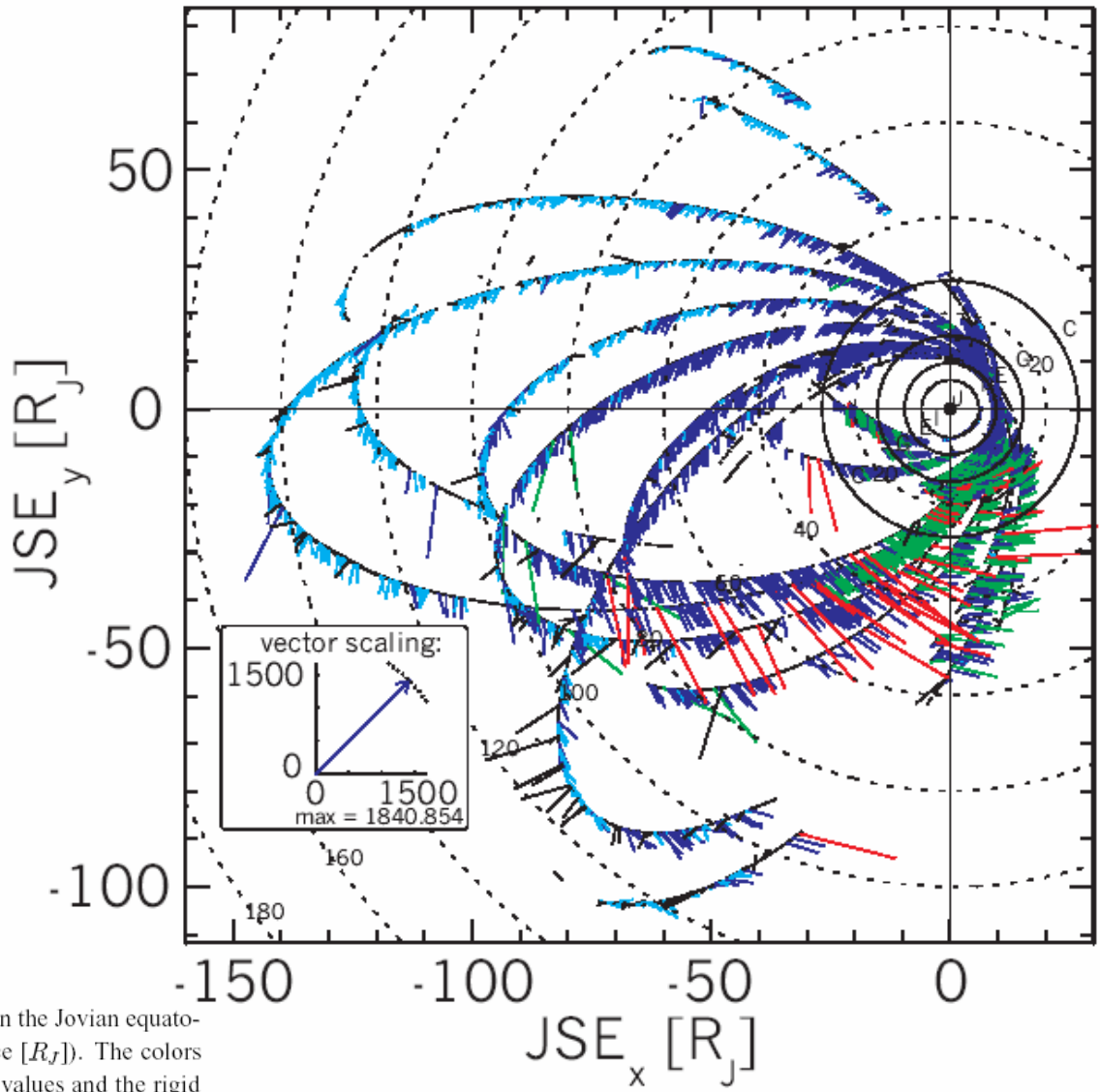


Figure 6. Flow velocity vectors of sulfur ions (16-30 keV/nucleon) in the Jovian equatorial plane. Data are dynamically time-averaged ($T = 3 \text{ min} \cdot \text{distance } [R_J]$). The colors distinguish between certain values of the ratio between the velocity values and the rigid corotation velocity v_{rigid} :

cyan: $v_{10}/v_{rigid} < 0.2$ (sub-corotational flow < 20%);

blue: $0.2 < v_{10}/v_{rigid} < 0.8$ (sub-corotational flow between 20 and 80%);

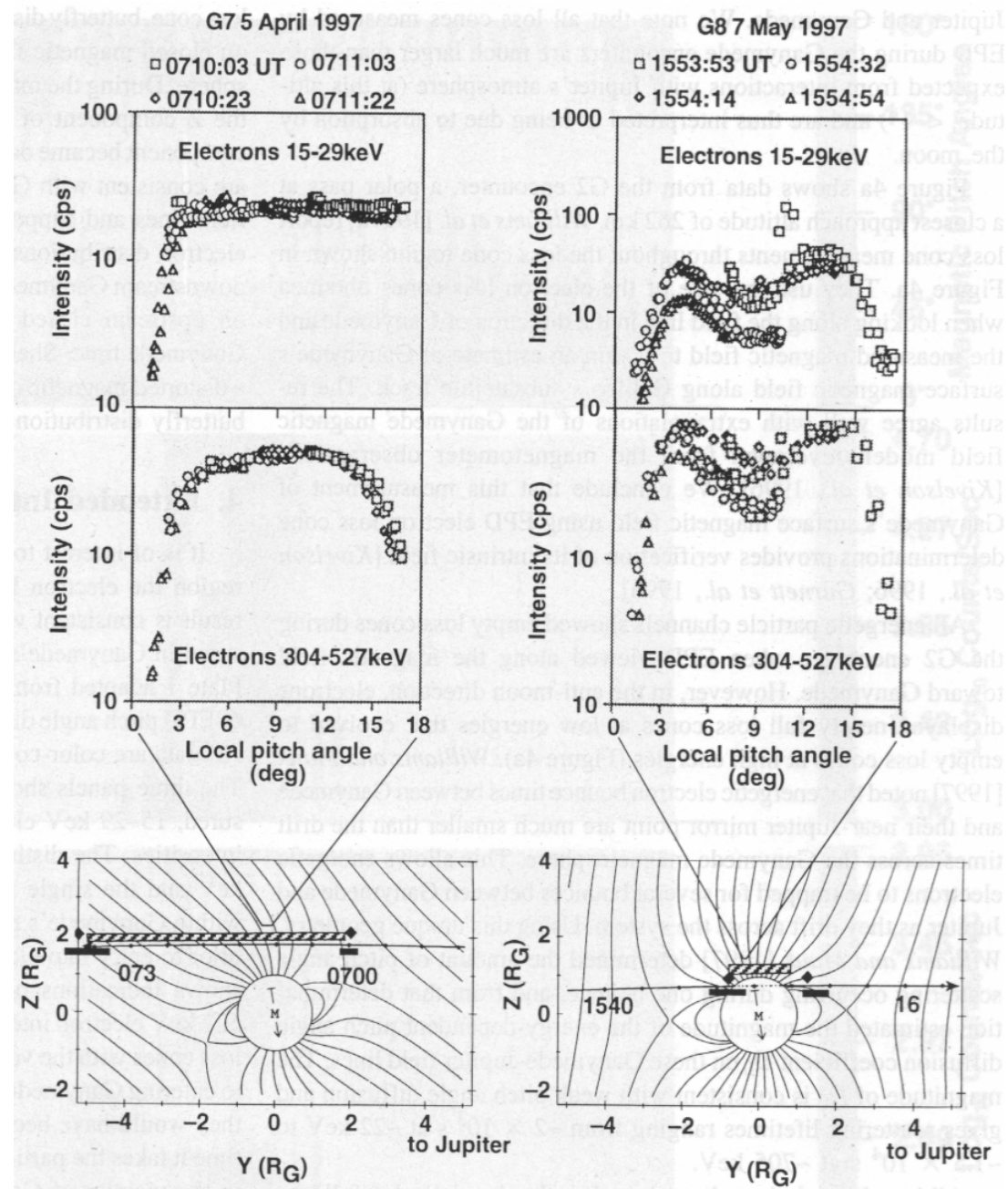
green: $0.8 < v_{10}/v_{rigid} < 1.2$ (corotational flow $\pm 20\%$);

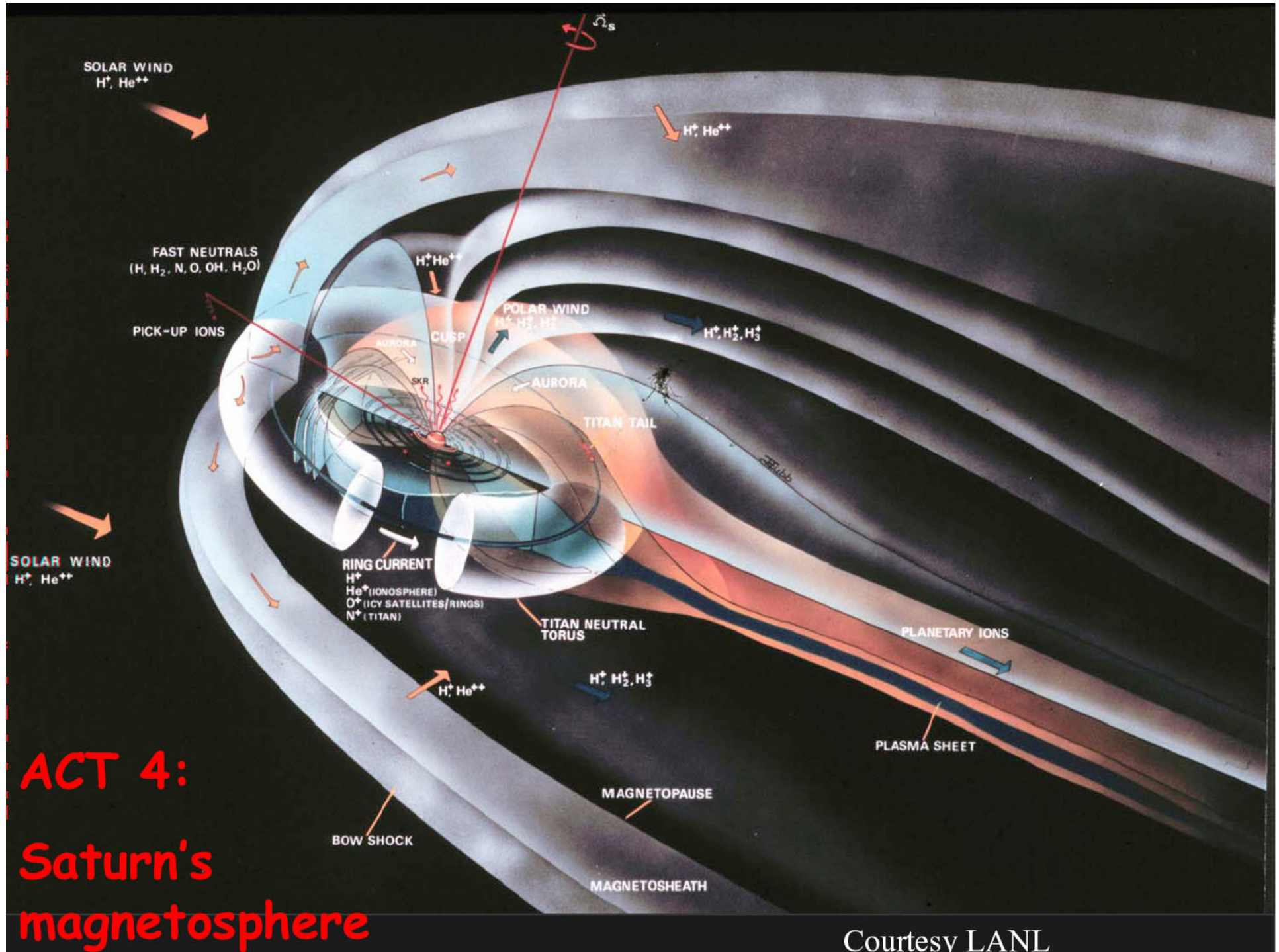
red: $v_{10}/v_{rigid} > 1.2$ (super-corotational flow).

Black vectors indicate those time periods where the radial components are larger than the components in corotation direction (radial inward and outward bursts).

Energetic electron measurements remotely diagnose magnetic topology, boundary geometry and surface magnetic field strengths of icy moons.

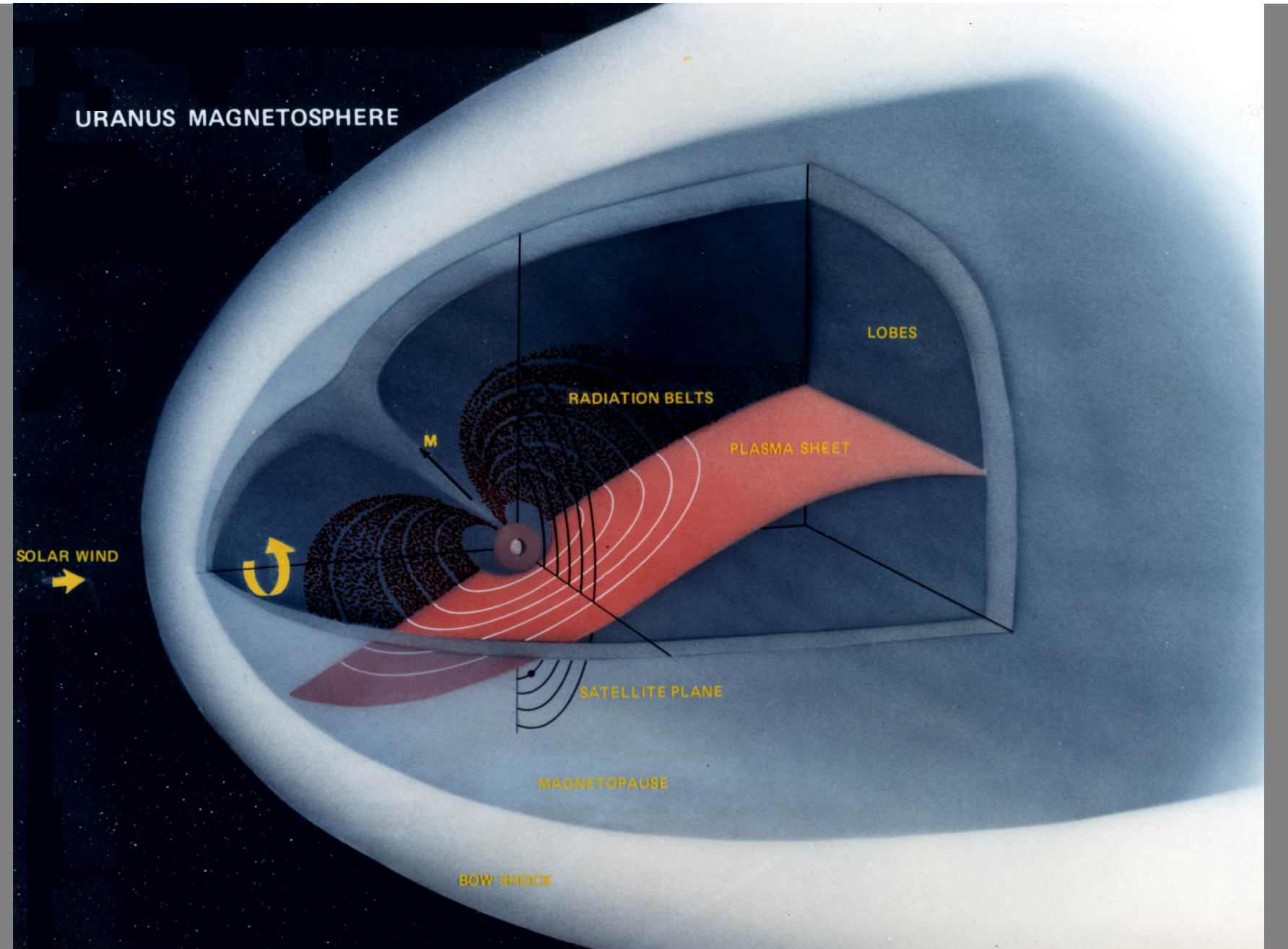
Williams et al., GRL, 1998





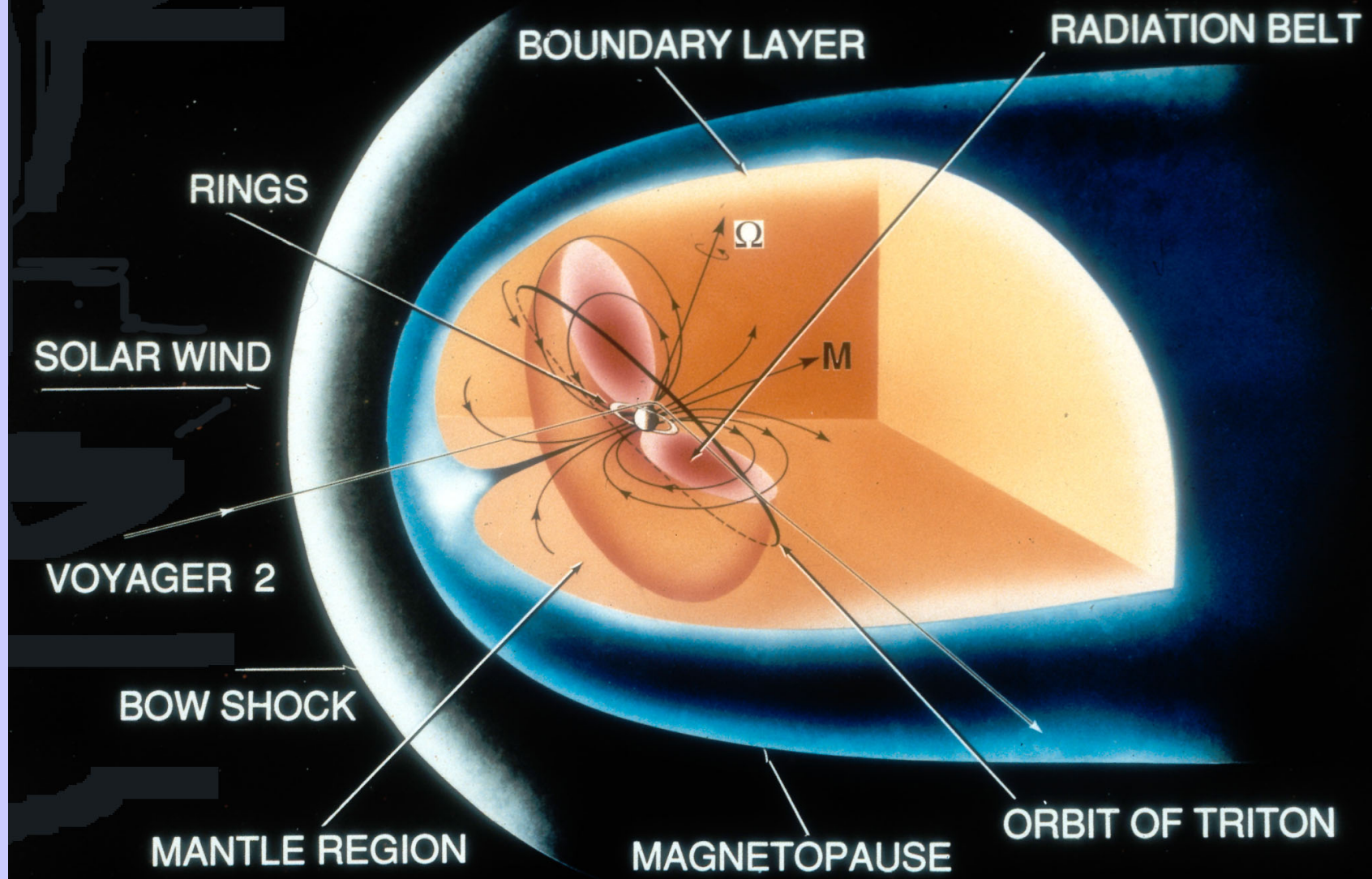
ACT 4: Saturn's magnetosphere

Courtesy LANL



Krimigis, Armstrong et al, *Science*, 233, 97-102, 1986

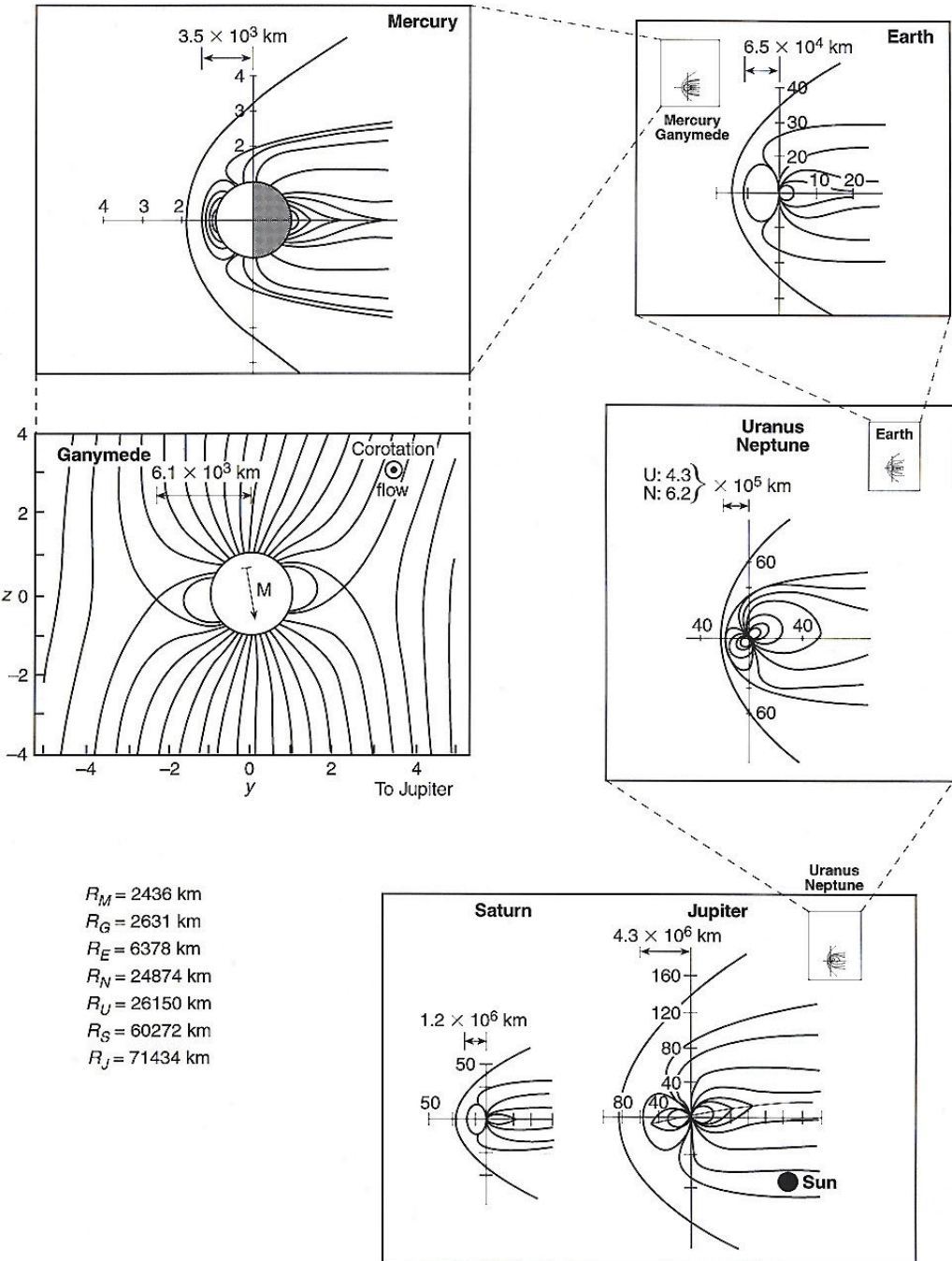
NEPTUNE'S MAGNETOSPHERE

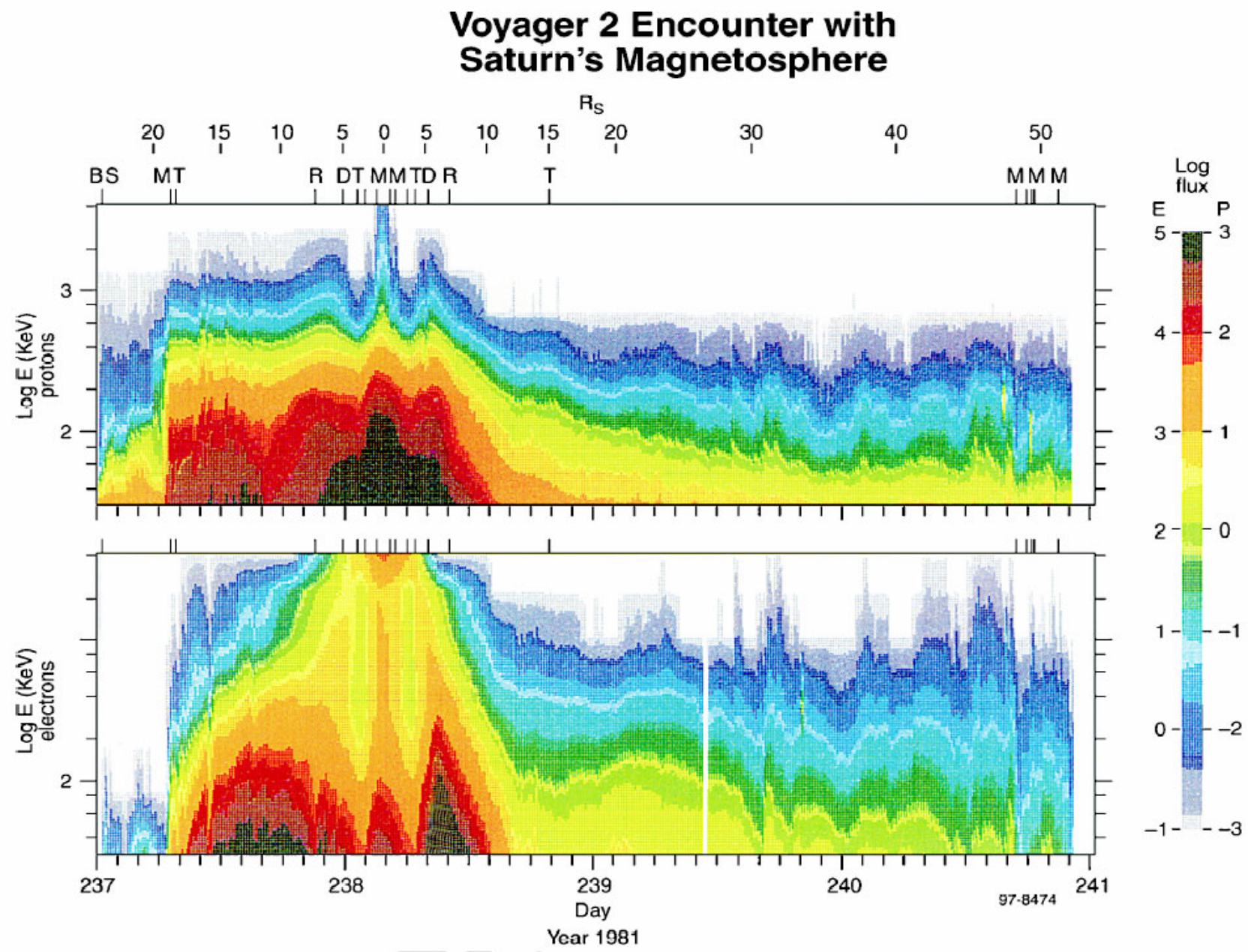


Krimigis, Armstrong et al, *Science*, 246, 1483-1494, 1989

Comparative Magnetospheres

(Williams, D. J., MOP,
JHU/APL, Laurel, 2002)





Van Allen Concept of Particle Absorption by Planetary Satellites

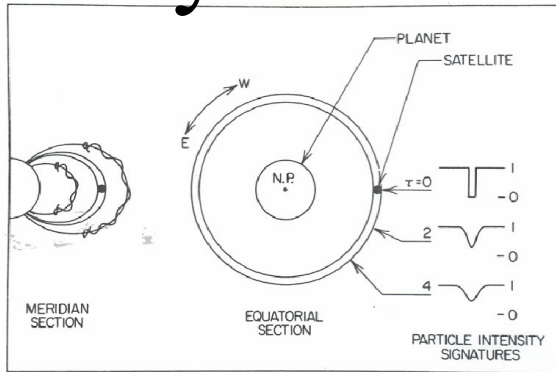


Fig. 22. Sketches illustrating the absorption by a planetary satellite of energetic charged particles trapped in the planet's magnetic field. The meridian section on the left shows the spiraling motion of charged particles between mirror points in opposite hemispheres and a tube of magnetic lines of force through the satellite (filled circle) that is depleted of particles. The equatorial section on the right shows the types of absorption signatures that may be observed as a spacecraft crosses the satellite's orbit at three different longitudes, i.e., as a function of the dimensionless parameter τ (Van Allen 1982).

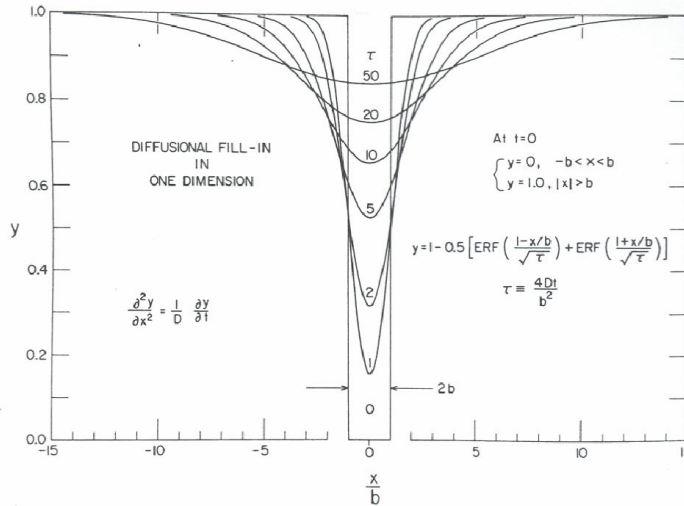


Fig. 23. A family of calculated curves illustrating the time dependence of the one-dimensional diffusive fill-in of the charged particle shadow of a satellite of radius b for particles whose radius of curvature is much less than b (Van Allen et al. 1980b).

Van Allen Concept of Resonant Energy

304

J. A. VAN ALLEN

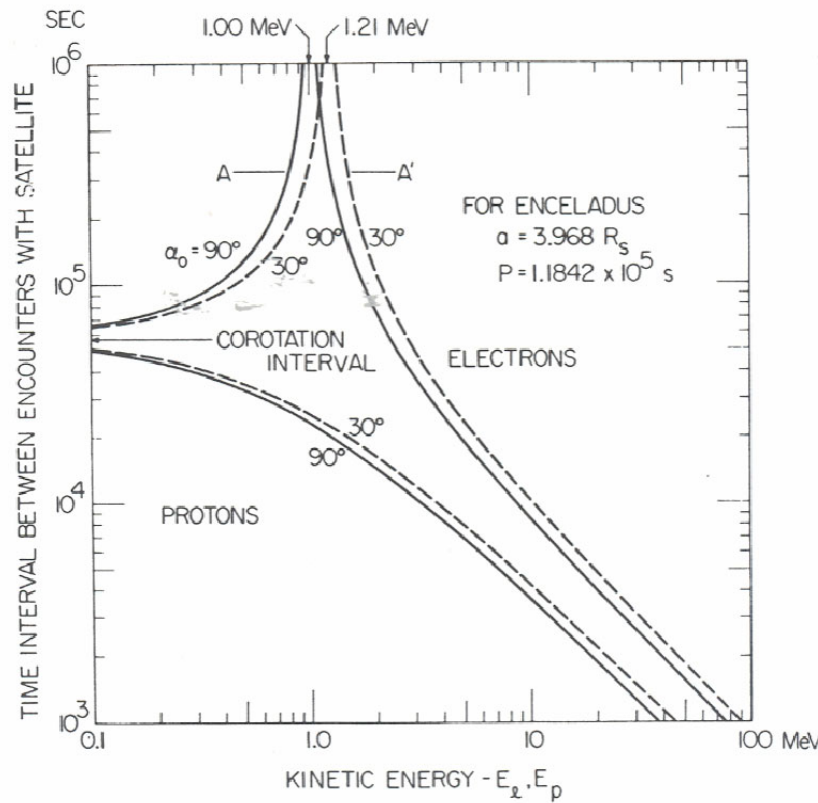
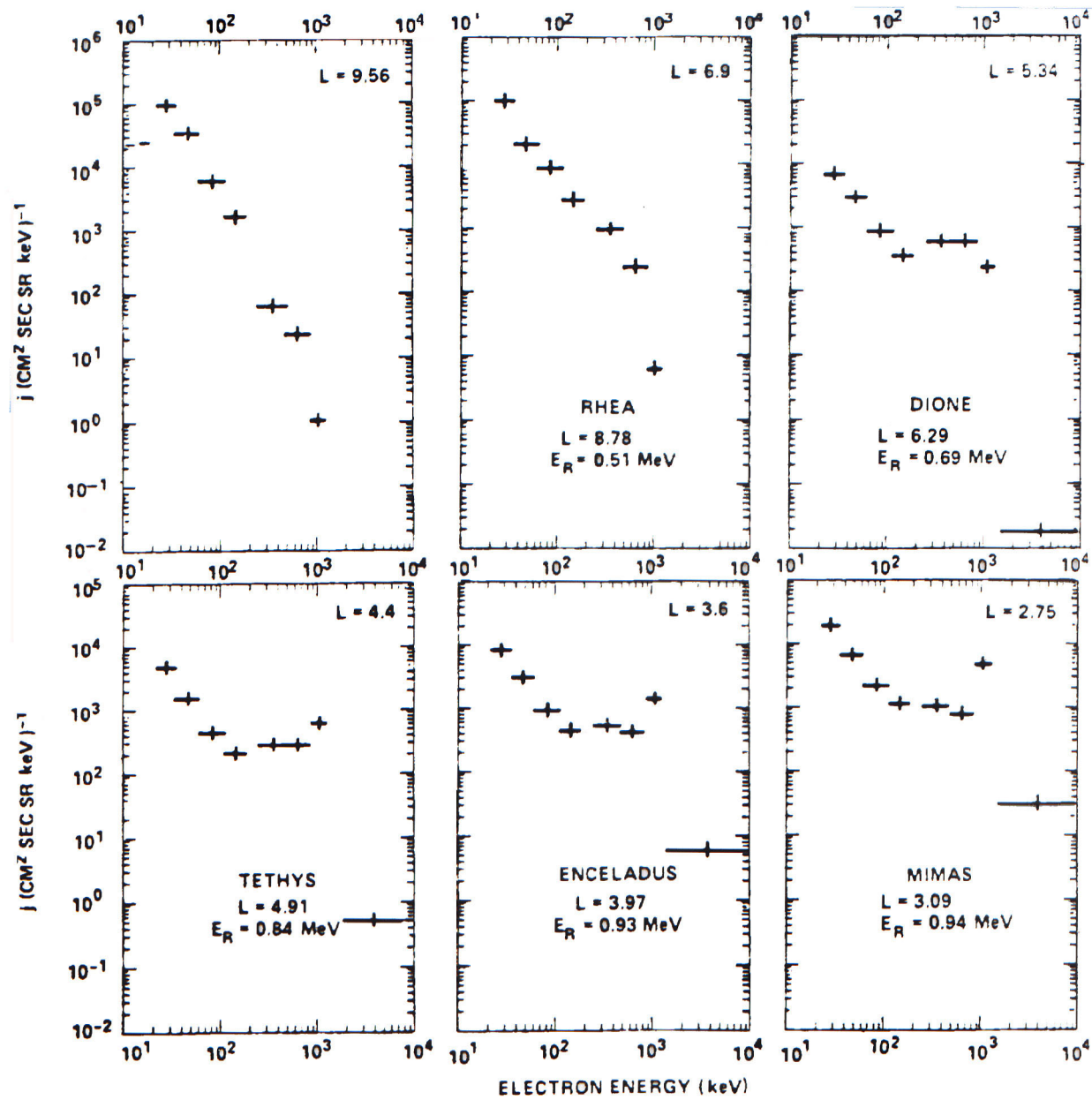
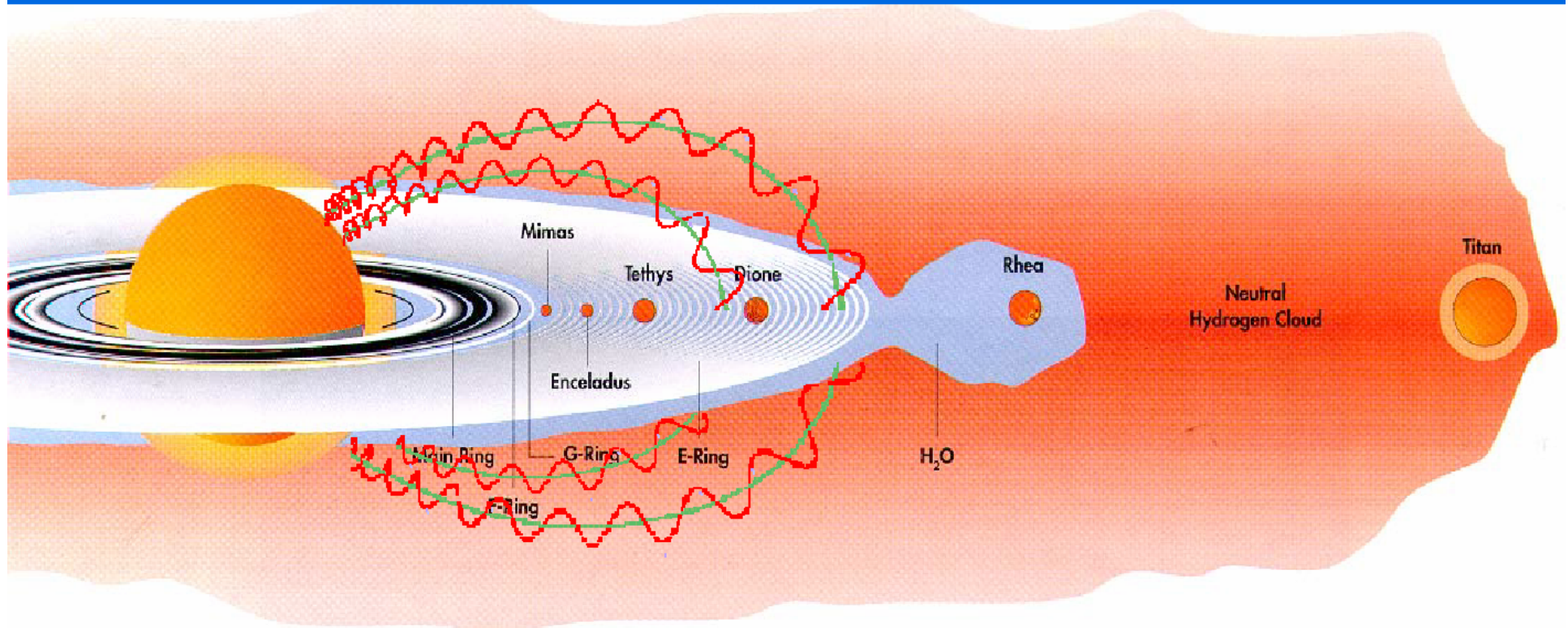


Fig. 17. Plots of the calculated time interval between successive encounters of electrons (upper two curves) and protons (lower two curves) with Enceladus as a function of kinetic energy of the particles. Of particular interest is the resonant, or synchronous, energy for electrons, $E_e = 1.00 \text{ MeV}$ for $\alpha_0 = 90^\circ$ and 1.21 MeV for $\alpha_0 = 30^\circ$ (cf. Table I herein using a slightly different magnetic field model than that used by the original authors). Protons experience no such resonance at any energy. The horizontal line AA' illustrates a sample diffusion time past Enceladus so as to result in a narrow band-pass filtering effect on the spectrum of electrons diffusing inward across its orbit ($1 R_S = 60,000 \text{ km}$ in this figure) (figure from Van Allen et al. 1980b).



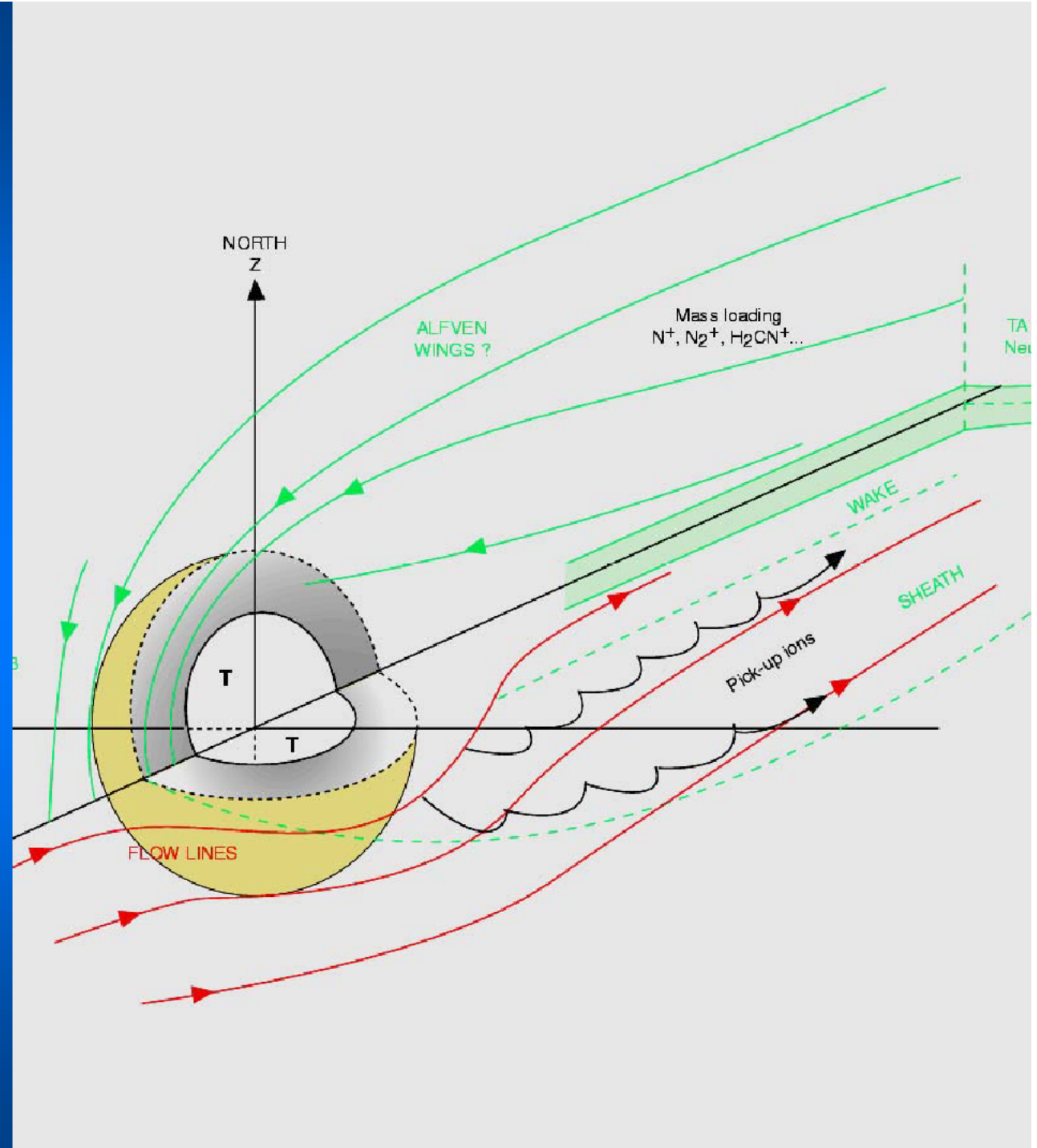
Krimigis, Armstrong et al, 1982

Interactions between phases in Saturn's magnetosphere

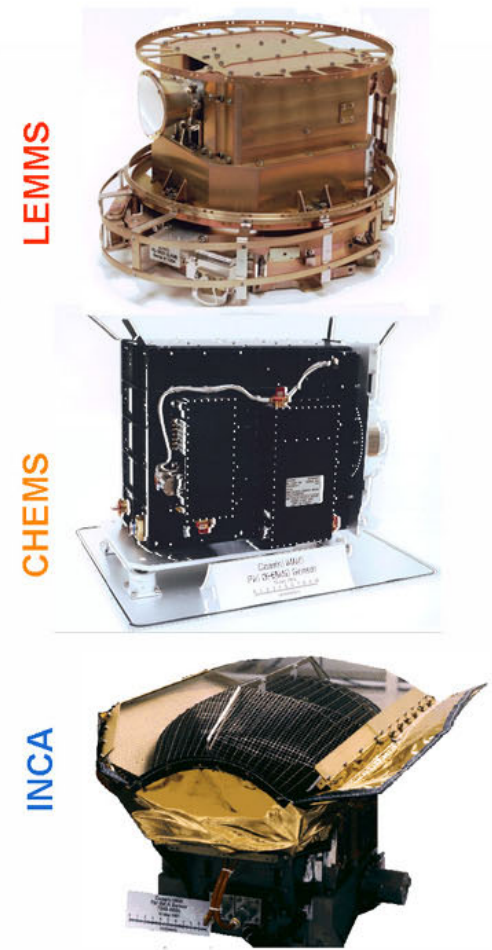
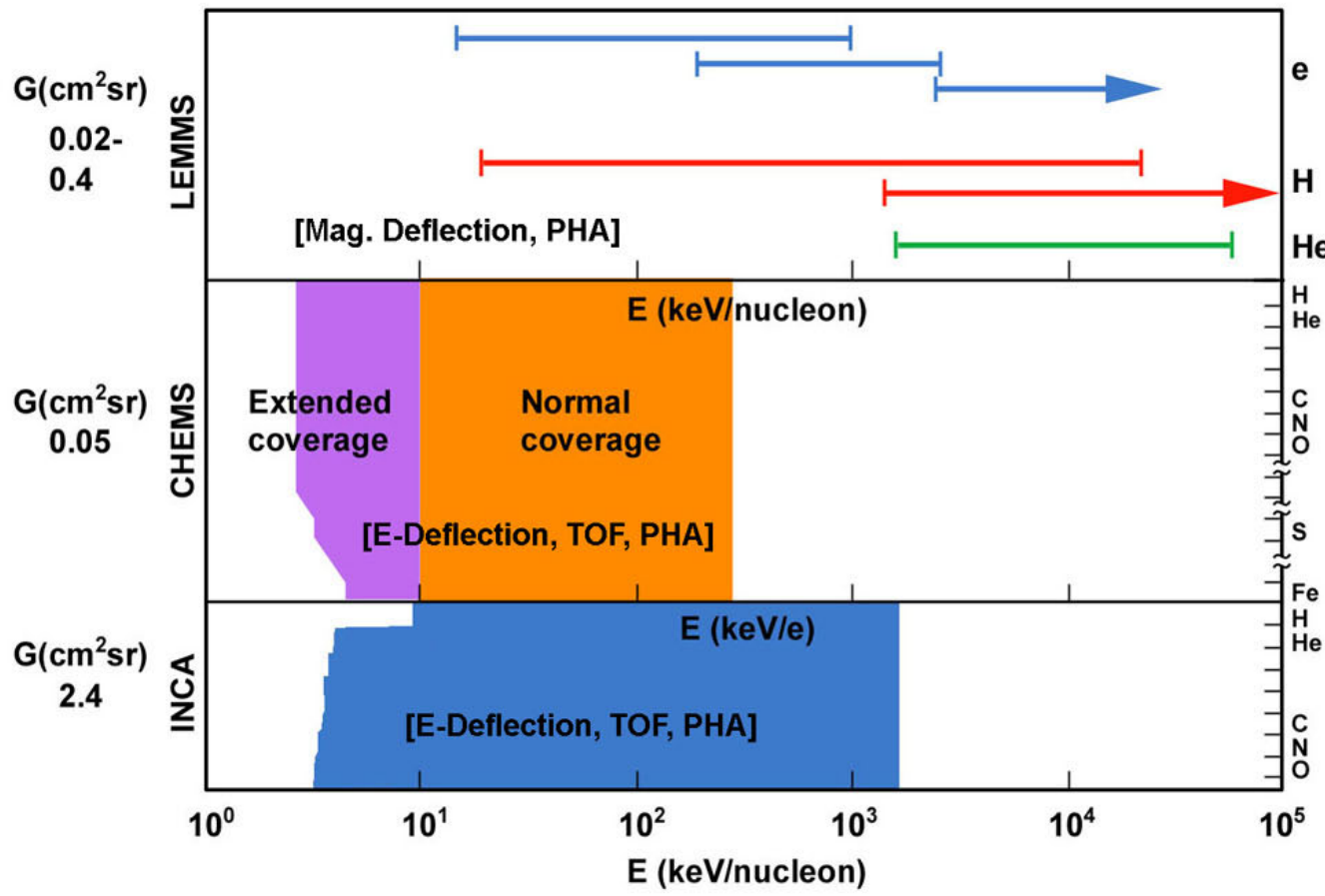


A possible 3-D
picture of the Titan
magnetospheric
interaction as
suggested by the
Voyager-1 fly-by and
by simulation studies.

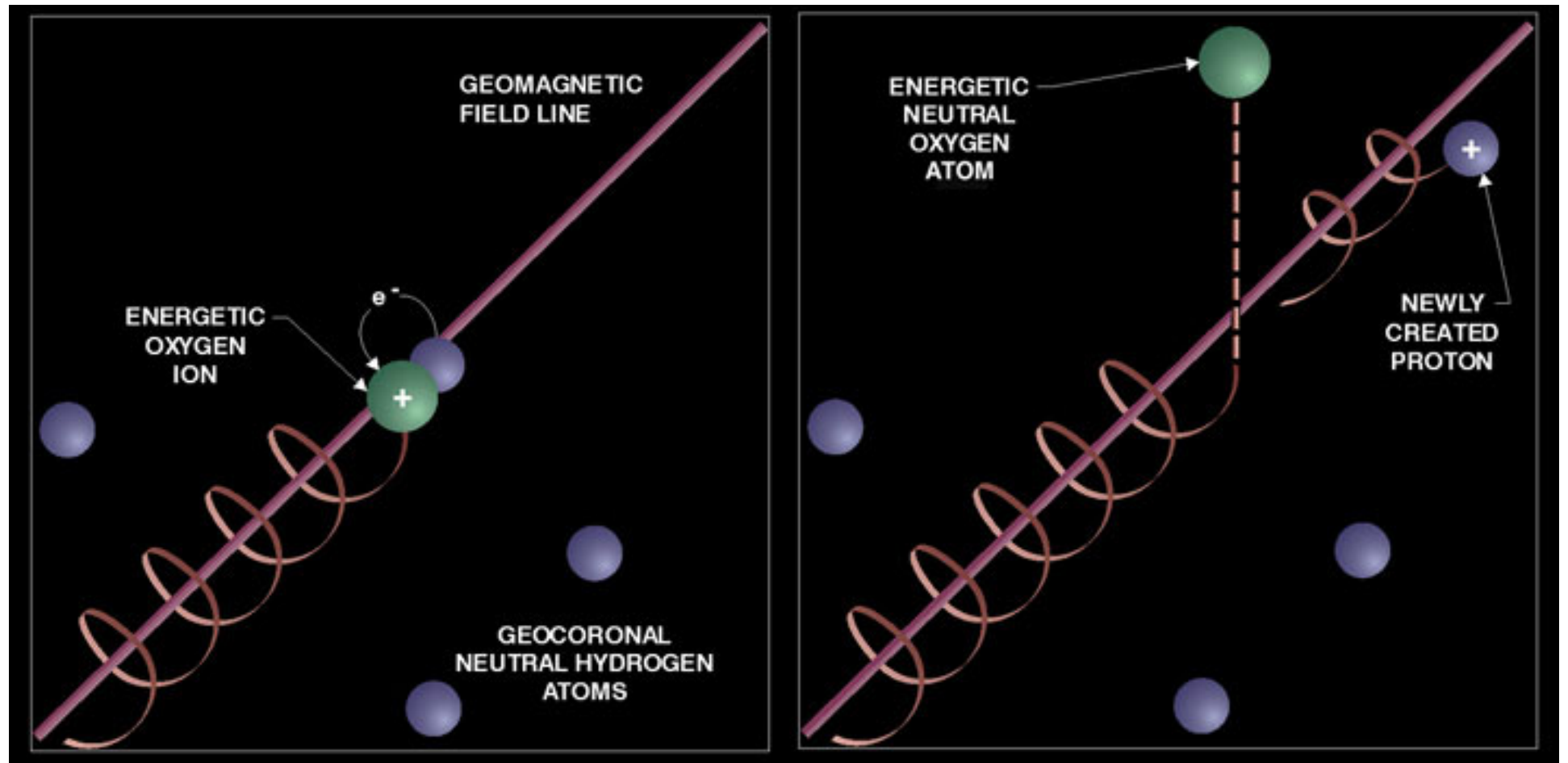
(Blanc, 2004)

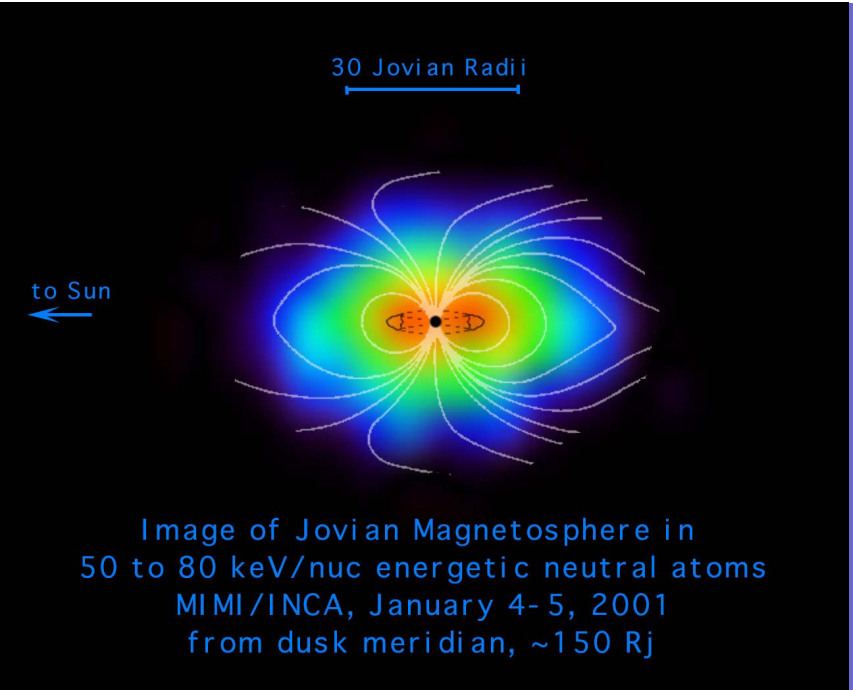


Magnetospheric Imaging Instrument (MIMI) On the Cassini Mission to Saturn/Titan

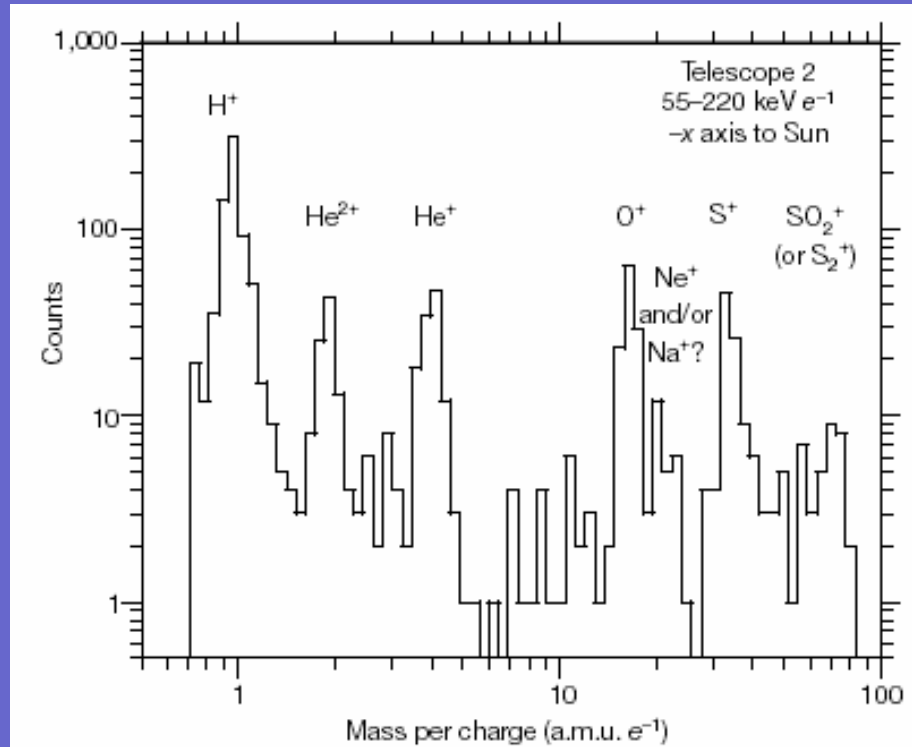
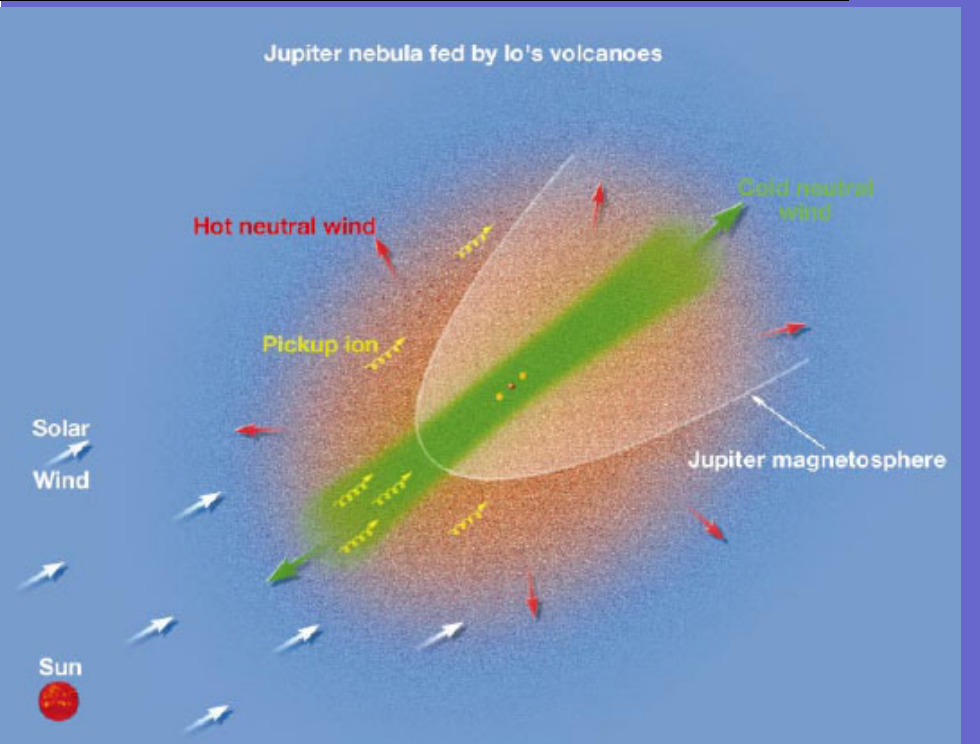


ENA Generation Mechanism



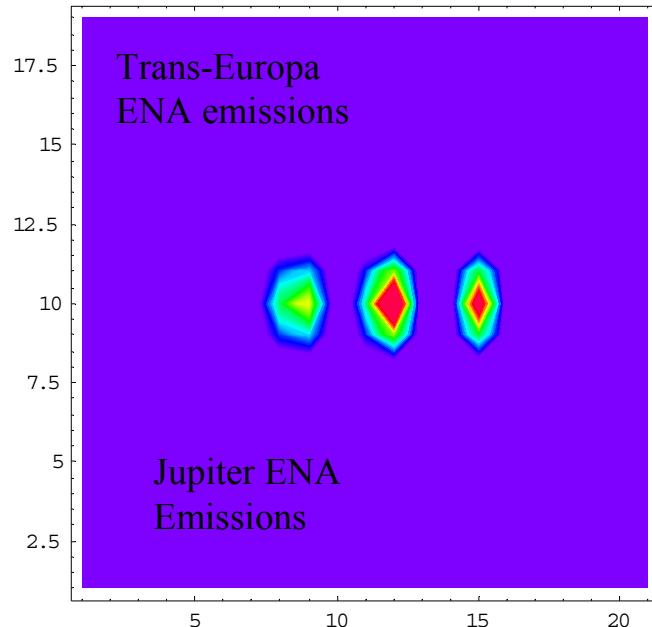


Cassini/MIMI discovery of
planetary nebula of Iogenic
gases populating huge
volume of space around
Jupiter (*Krimigis et al,*
Nature, 415, 994, 2002)

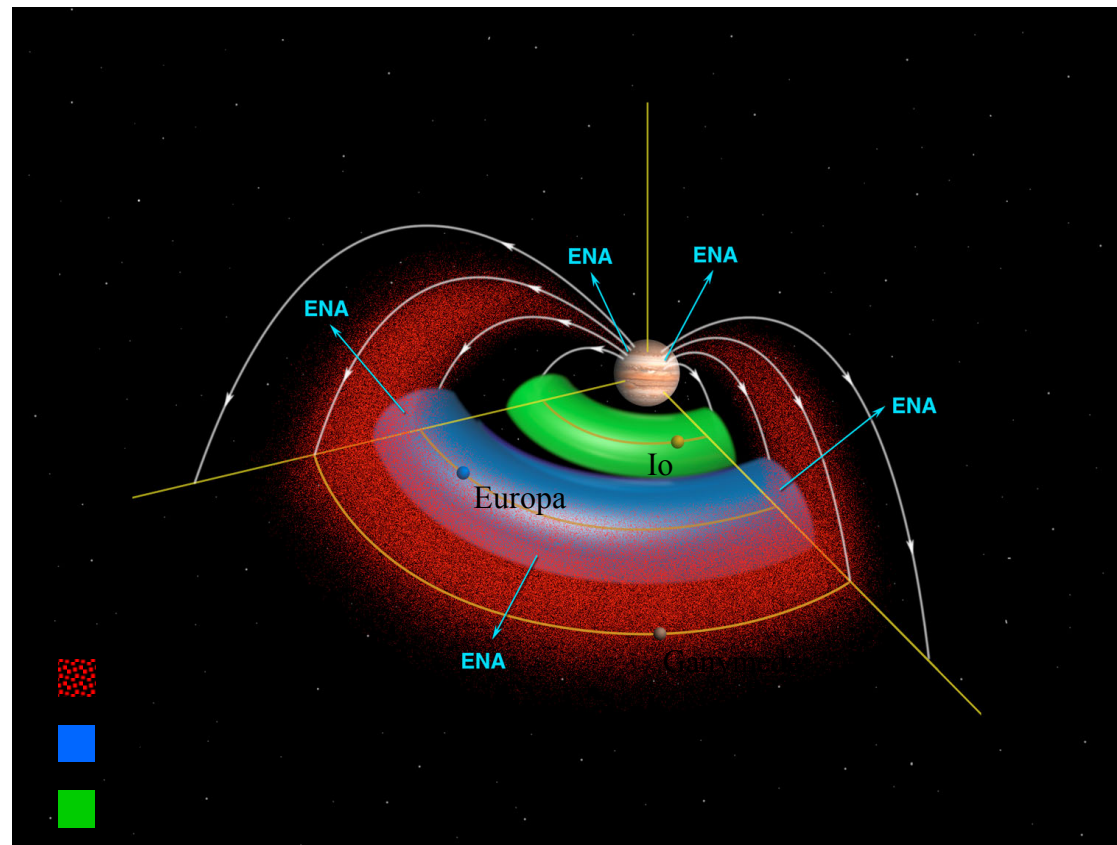


Cassini Ion and Neutral Camera (INCA) Discovers Massive Gas Cloud Encircling Jupiter

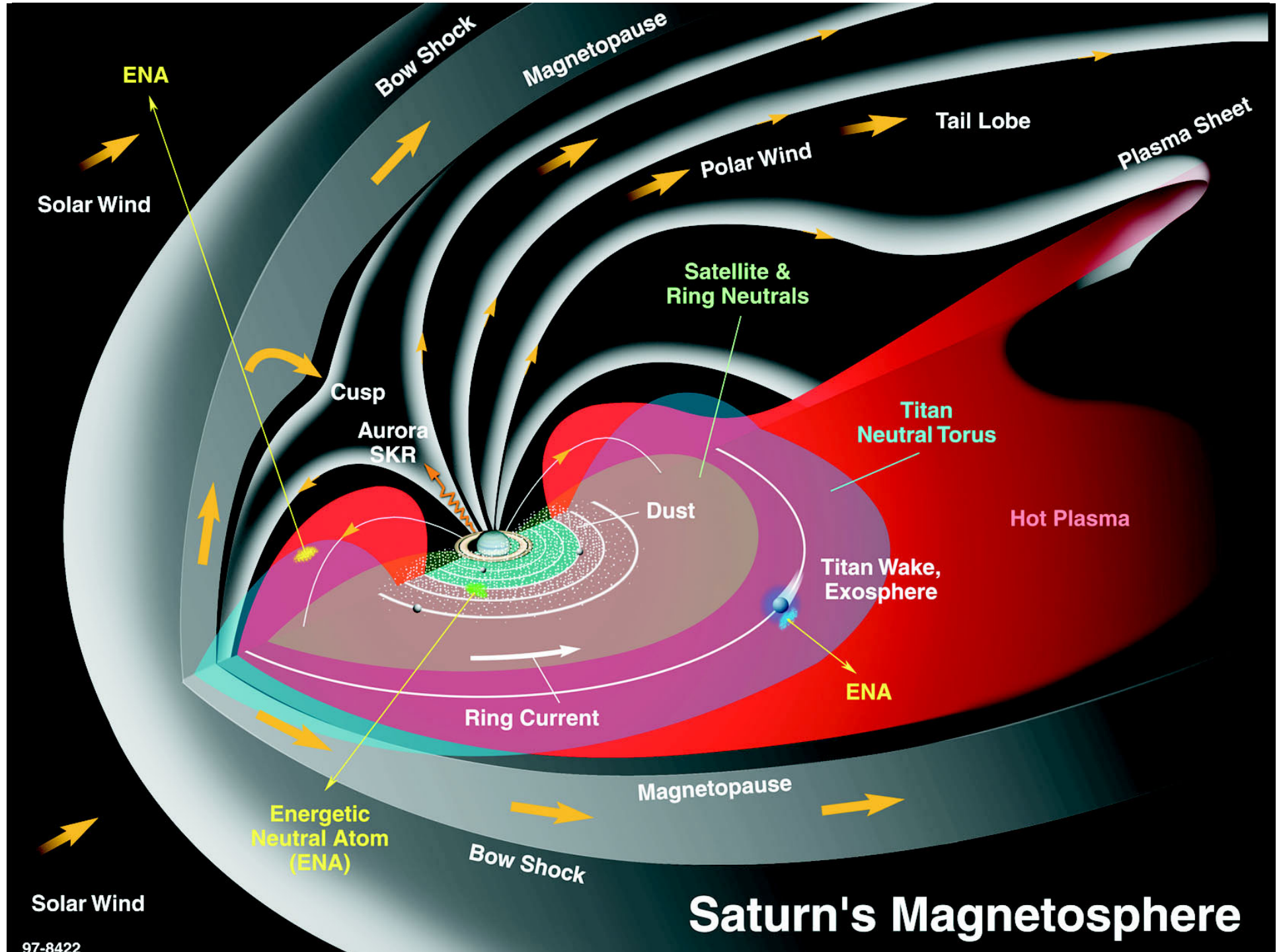
Planetary space environments glow with Energetic Neutral Atoms (ENAs) from interactions between magnetically trapped hot ions and cold neutral gas



INCA ENA Image of Jupiter reveals torus of gas just outside the orbit of Jupiter's moon Europa
(Mauk, Mitchell, Krimigis, and Roelof, Nature, 421, 920-922, 2003)



Configuration of Jupiter's space environment as inferred from the INCA image. The new component is the blue gas torus



CASSINI MAPS INSTRUMENTS

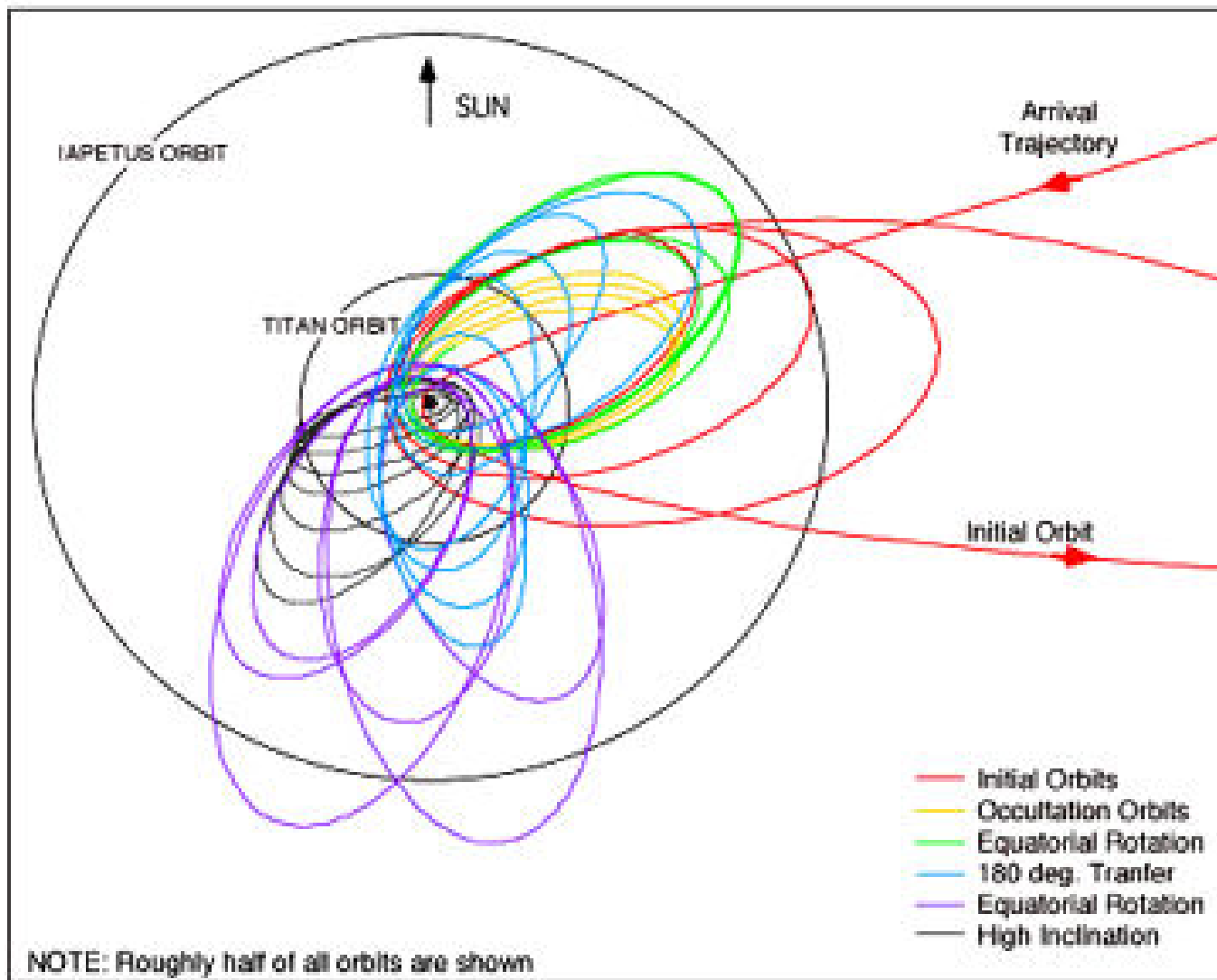
In Situ

Remote sensing

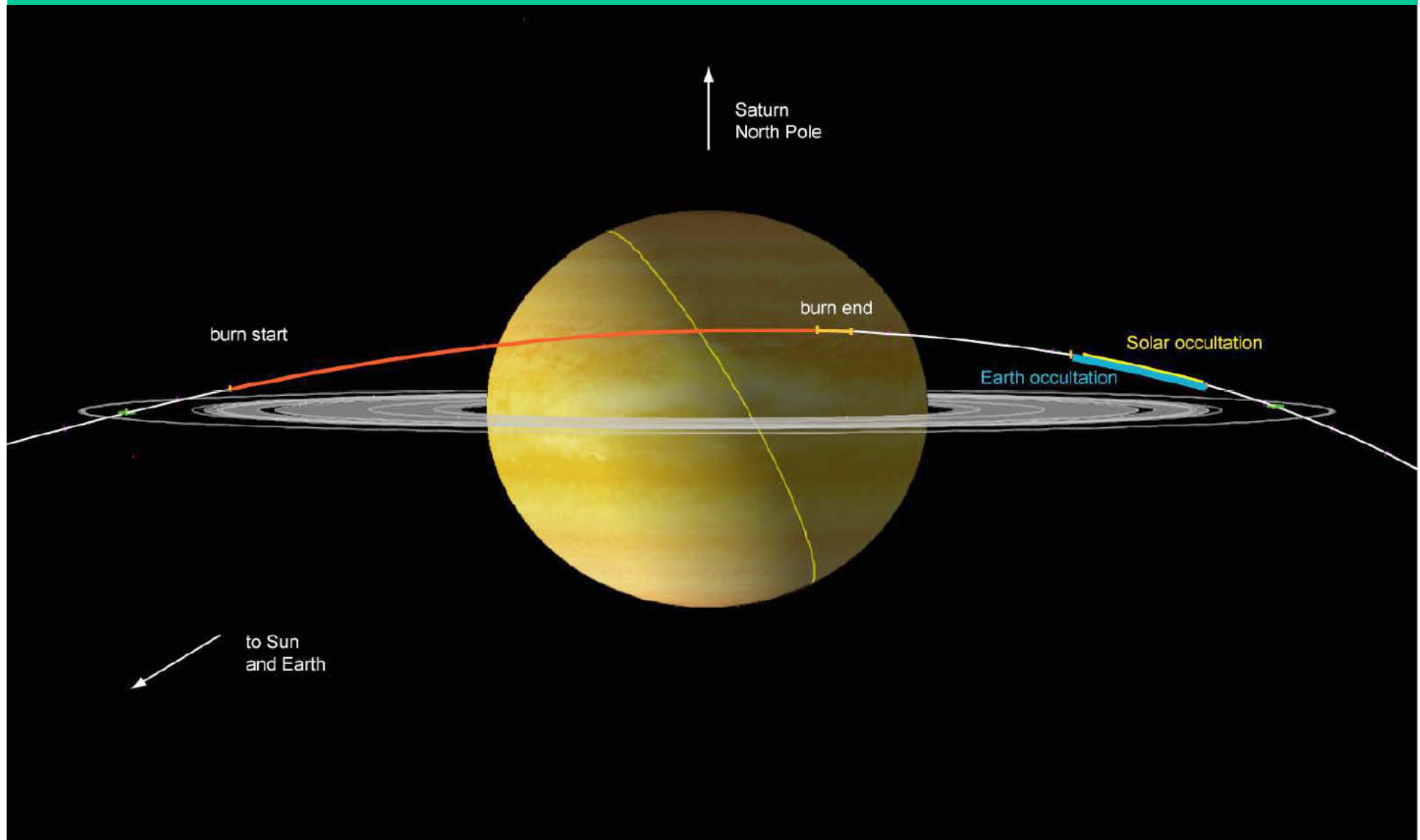
CAPS	Cassini Plasma Spectrometer (D.T. Young)	F(v), composition, density, velocity and temperature of ions and electrons	
CDA	Cosmic Dust Analyzer (E. Grün)	Flux, velocity, charge, mass and composition of dust and ice particles	
INMS	Ion and Neutral Mass Spectrometer (J.H. Waite)	Measures neutral species and low-energy ions	
MAG	Dual Technique Magnetometer (D. Southwood)	Direction and strength of magnetic field	
MIMI	Magnetospheric Imaging Instrument (S.M. Krimigis)	Composition, charge state and energy distribution of energetic ions and electrons	ENA imaging of Saturn's magnetosphere and Titan's environment
RPW S	Radio and Plasma Wave Science (D.A. Gurnett)	Local plasma waves plus electron density and temperature	Radio emissions
RSS	Radio Science Subsystem (A.J. Kliore)	Ionosphere density profiles of Saturn and Titan	
UVIS	Ultraviolet Imaging Spectrograph (L.W. Esposito)		Ultraviolet emissions (aurora, airglow)
ISS	Imaging Science Subsystem (C. Porco)		Imaging of aurora, all Saturn system objects
VIMS	Visible and Infrared Mapping Spectrometer (R. Brown)		Imaging and spectroscopy of IR aurora

CASSINI - SATURN ORBITAL SAMPLE TOUR

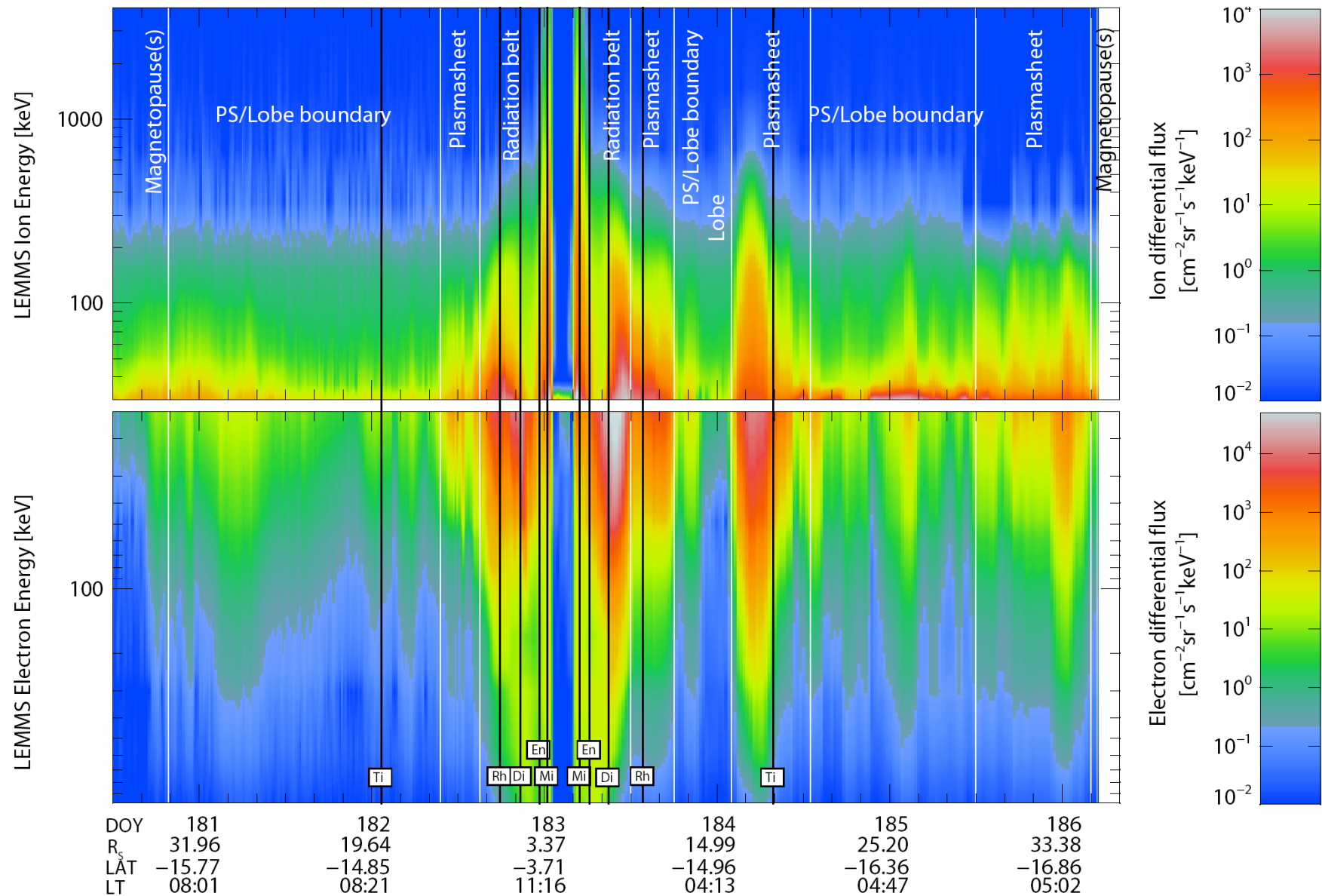
Saturn North Pole View



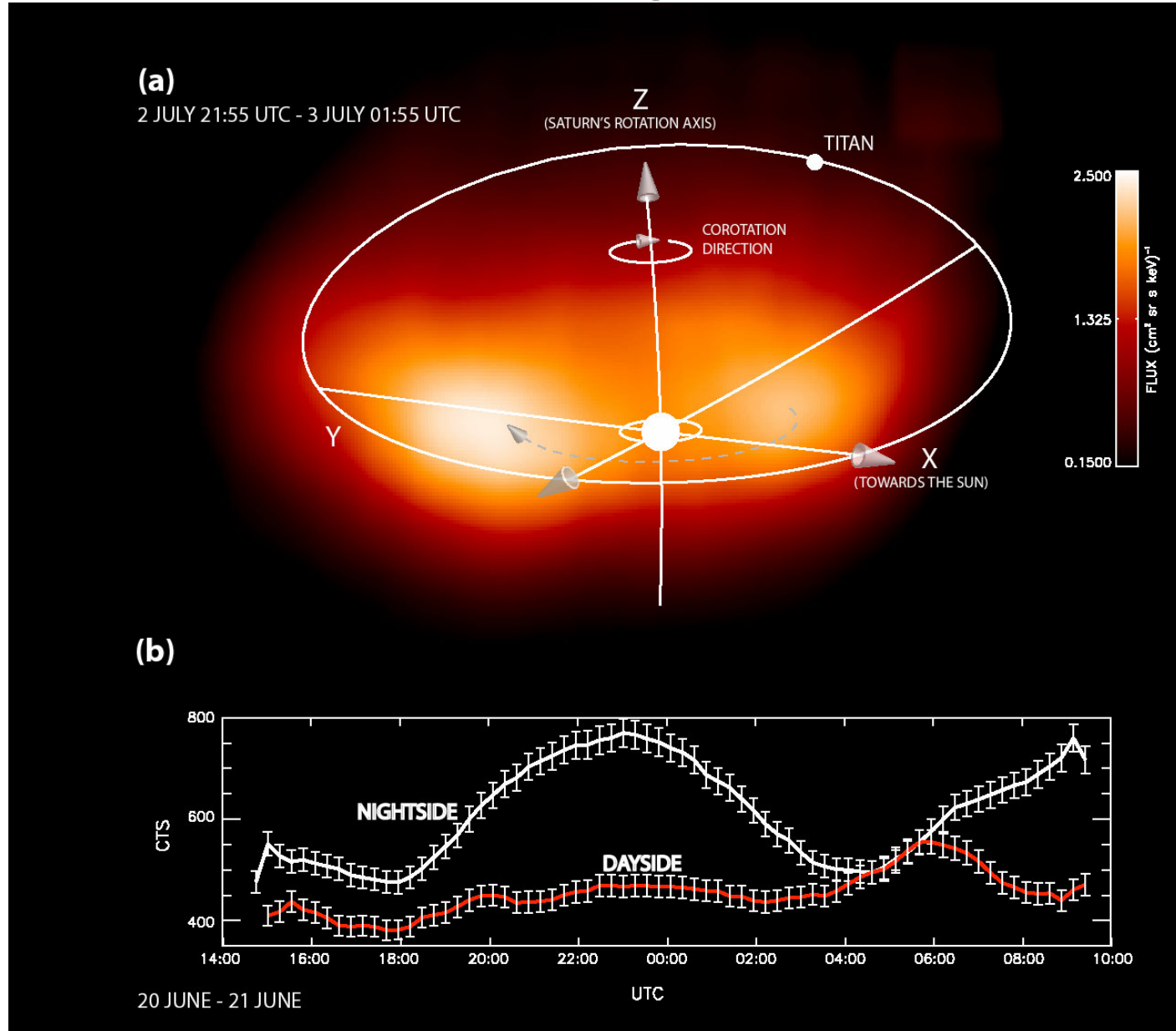
Cassini SOI Geometry



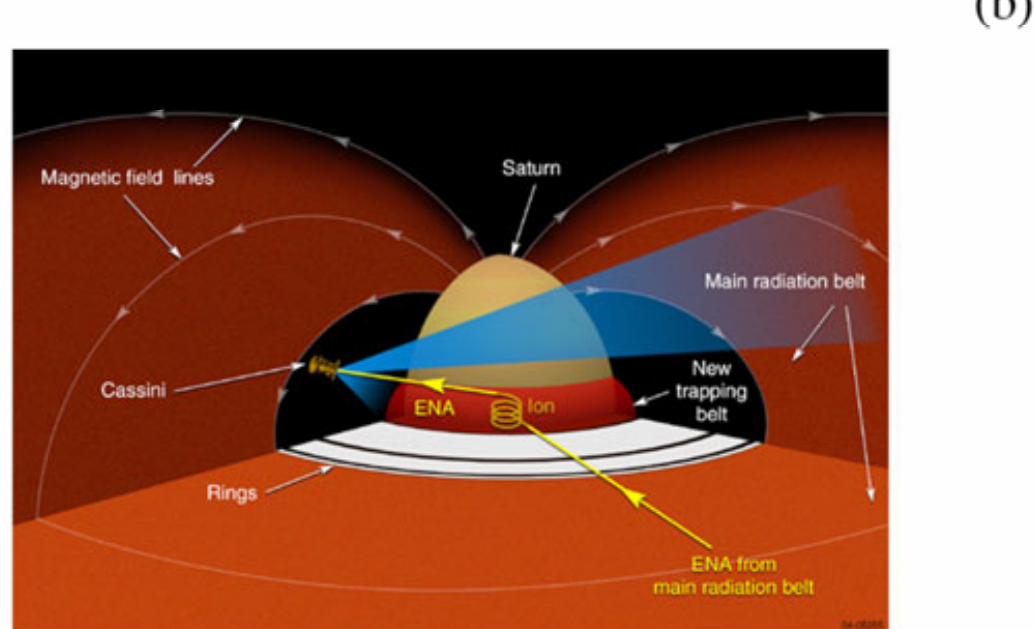
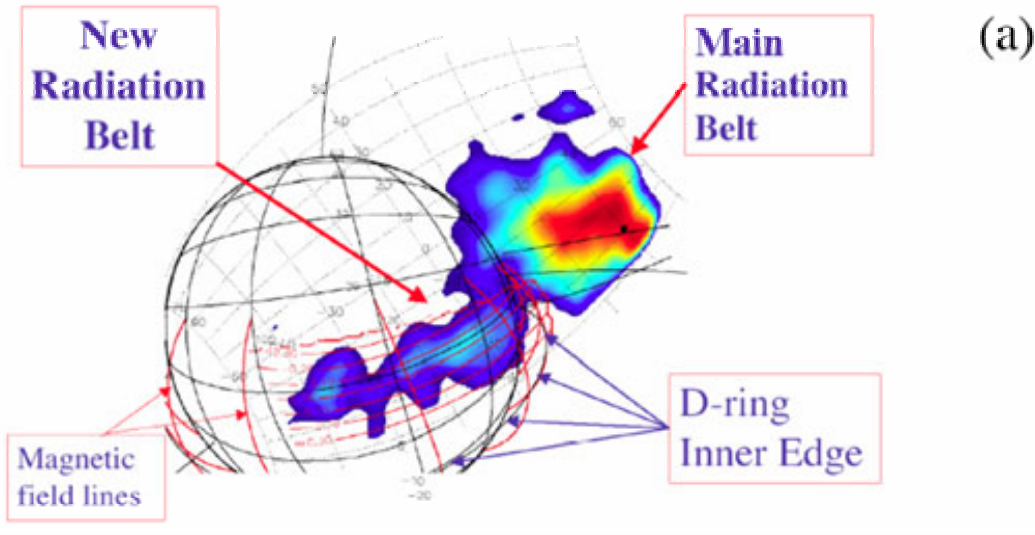
Cassini/MIMI/LEMMS In Situ Measurements



Imaging the Corotating Magnetosphere of Saturn through ENA

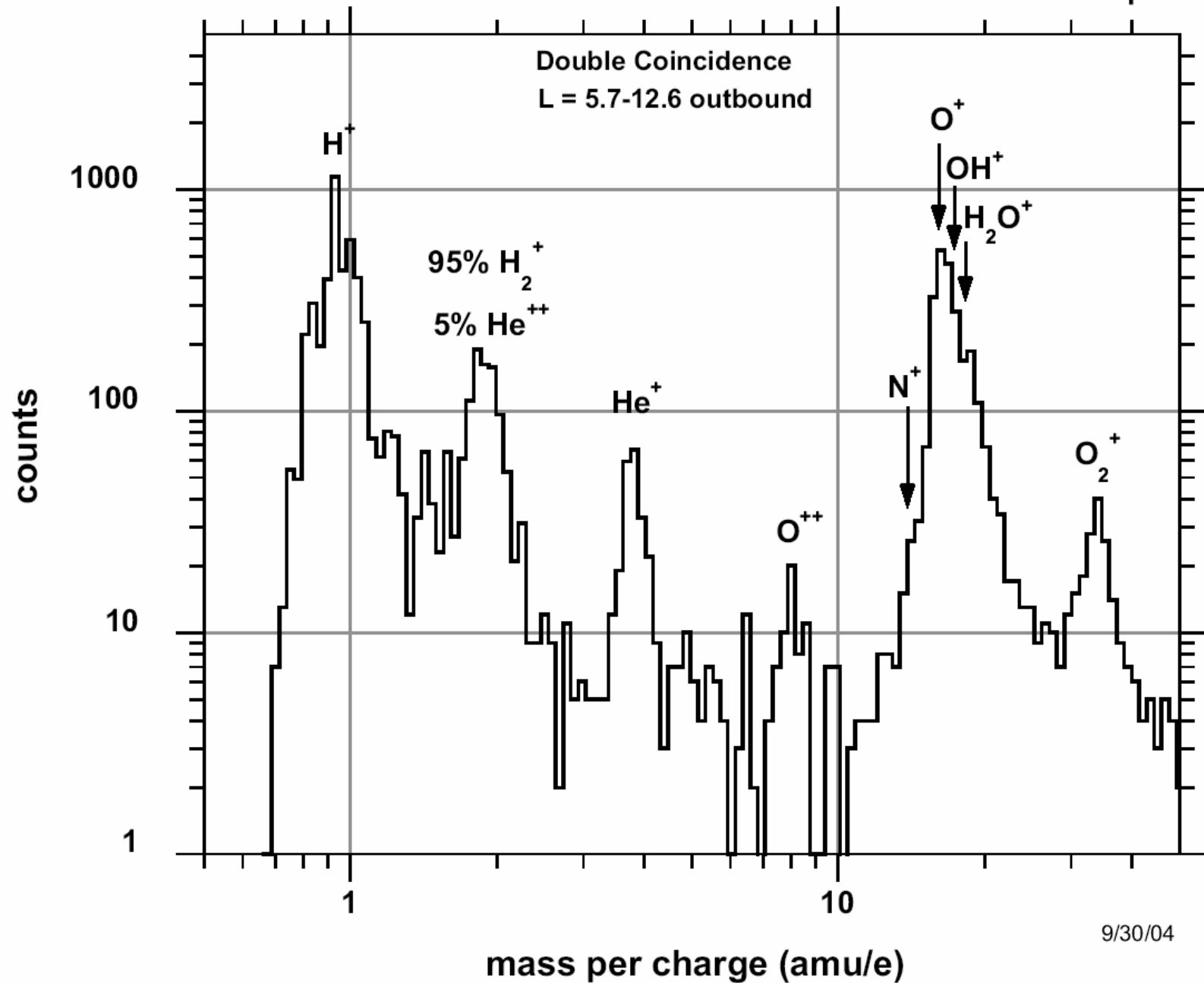


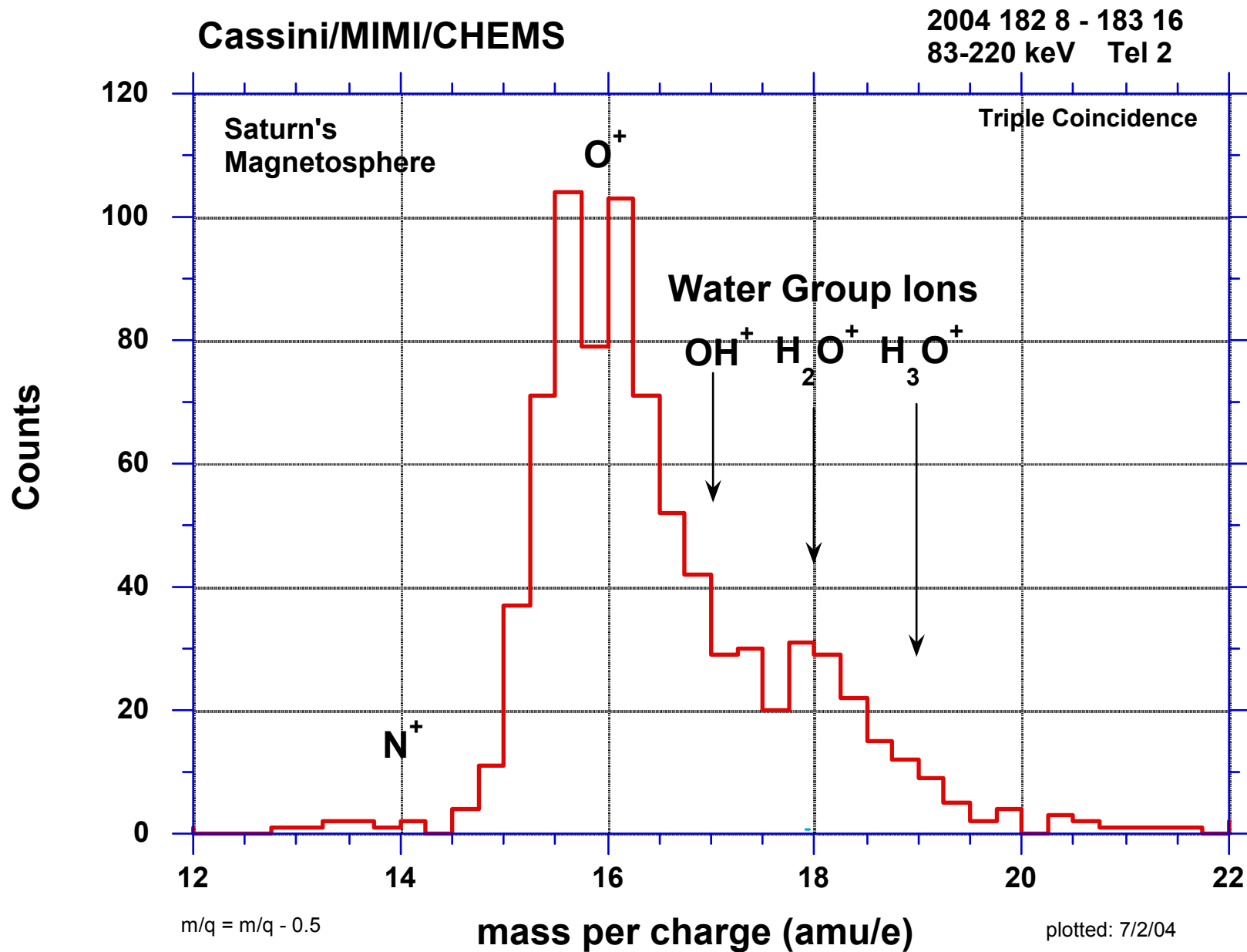
Radiation Belt Inward of D-Ring



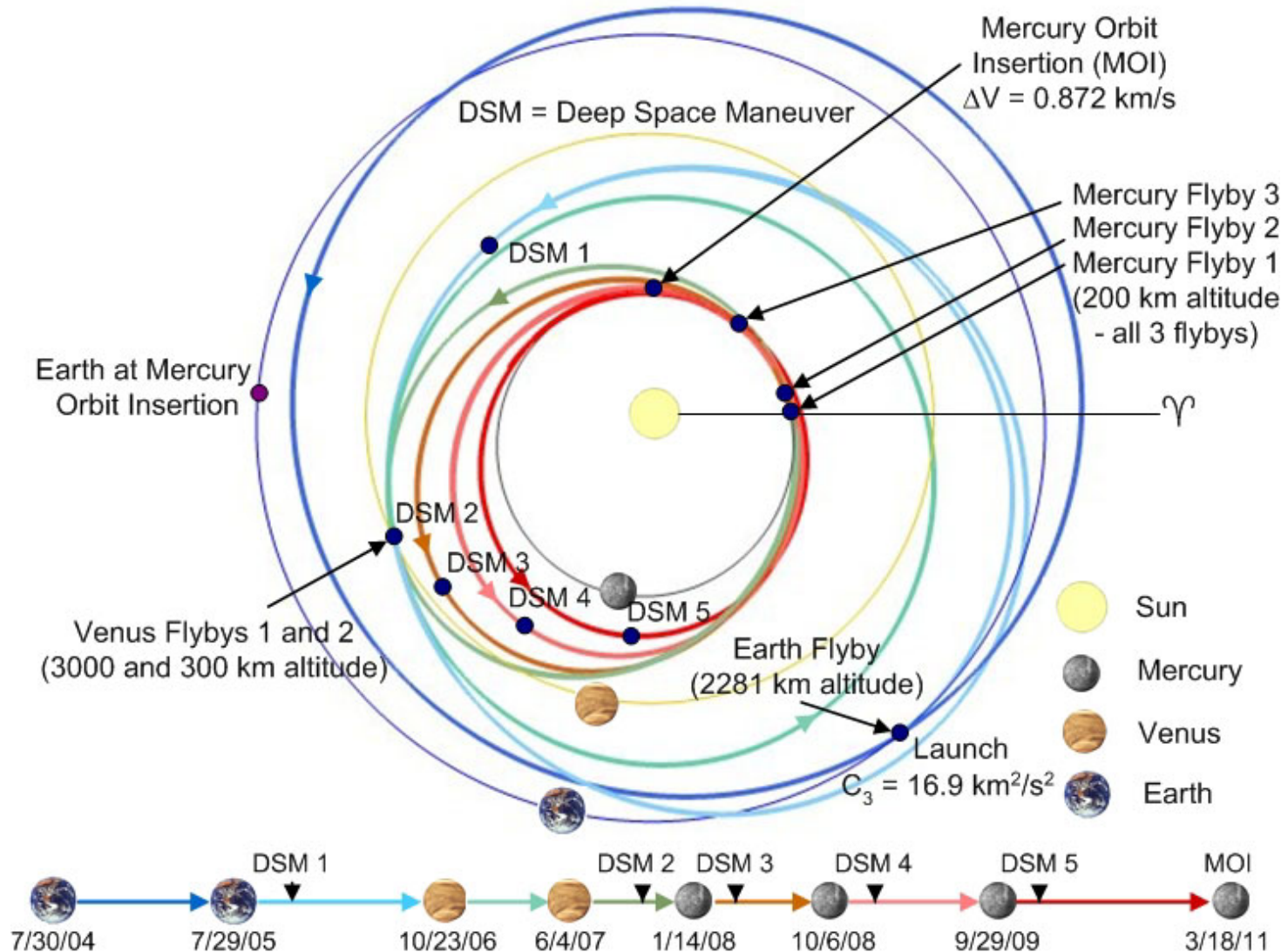
Cassini/MIMI/CHEMS

2004 183 0800-1800
83-220 keV/e All Telescopes





Trajectory



NEW HORIZONS:

Shedding Light on Frontier Worlds



Concept Study Report for
the Pluto-Kuiper Belt Mission
NASA AO-OSS-01

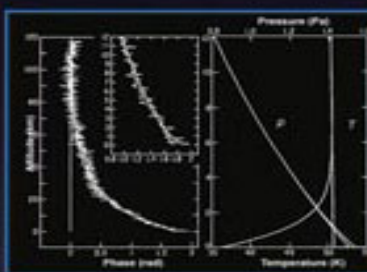
Principal Investigator:
S. Alan Stern
Southwest Research Institute



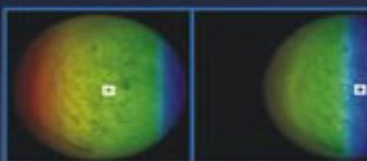
Global
Mapping &
High-Res
Imagery



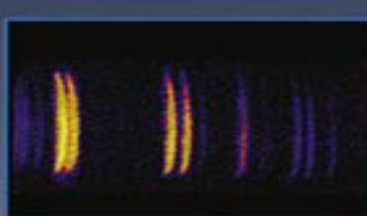
Radio Science
Occultation,
Gravity, &
Radiometry



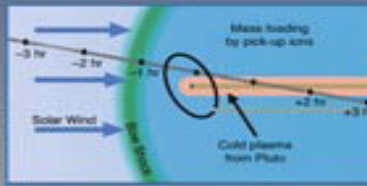
IR Surface
Composition &
Temperature
Mapping



UV Airglow &
Occultation
Imaging
Spectroscopy



In Situ Particles
& Plasma
Measurements



Stern-4
01-0890-2

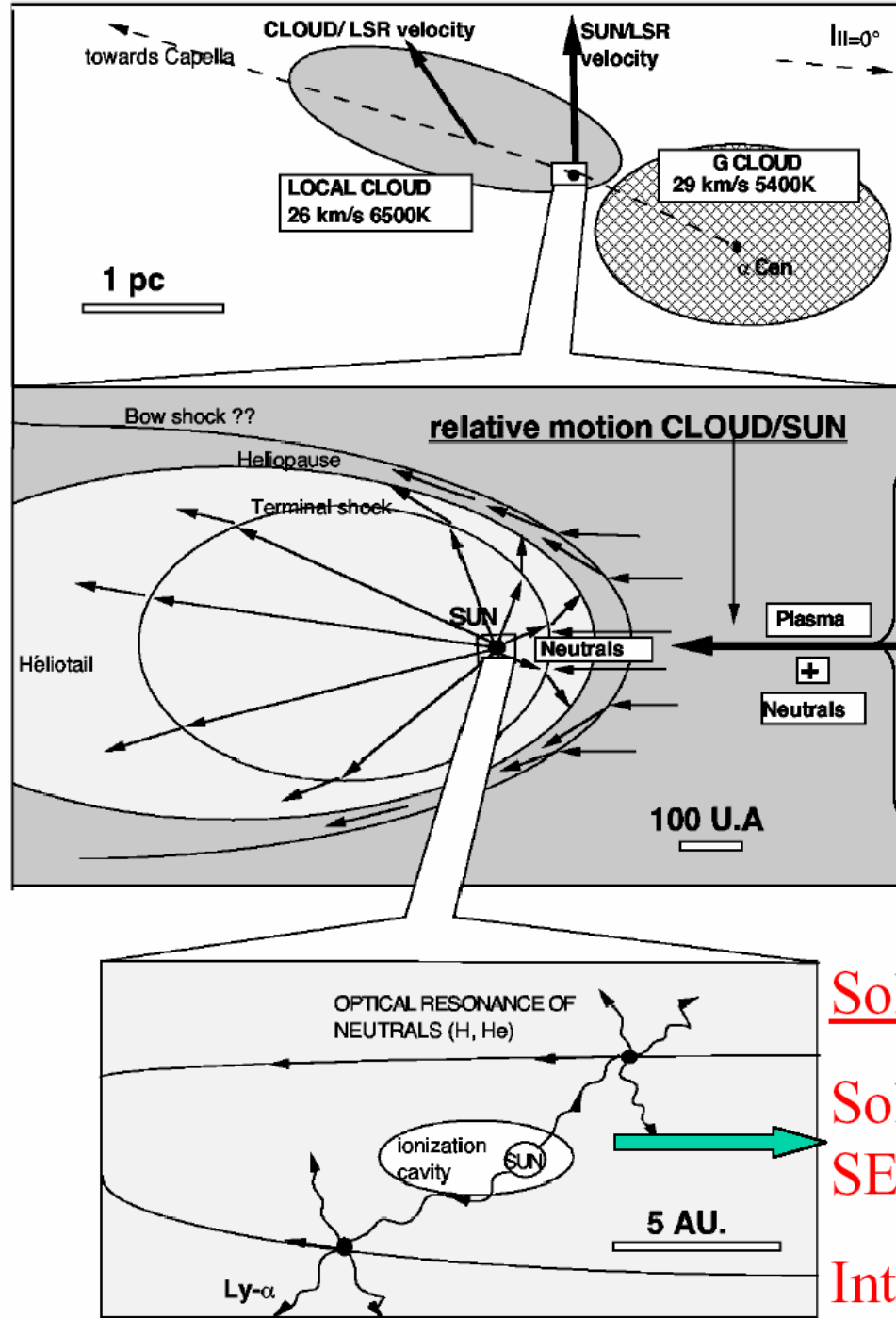
Launch in
January,
2006.

Pluto arrival
in July,
2015

Interaction products:

- Pick-up ions
- Energetic neutrals
- Anomalous CR's ?

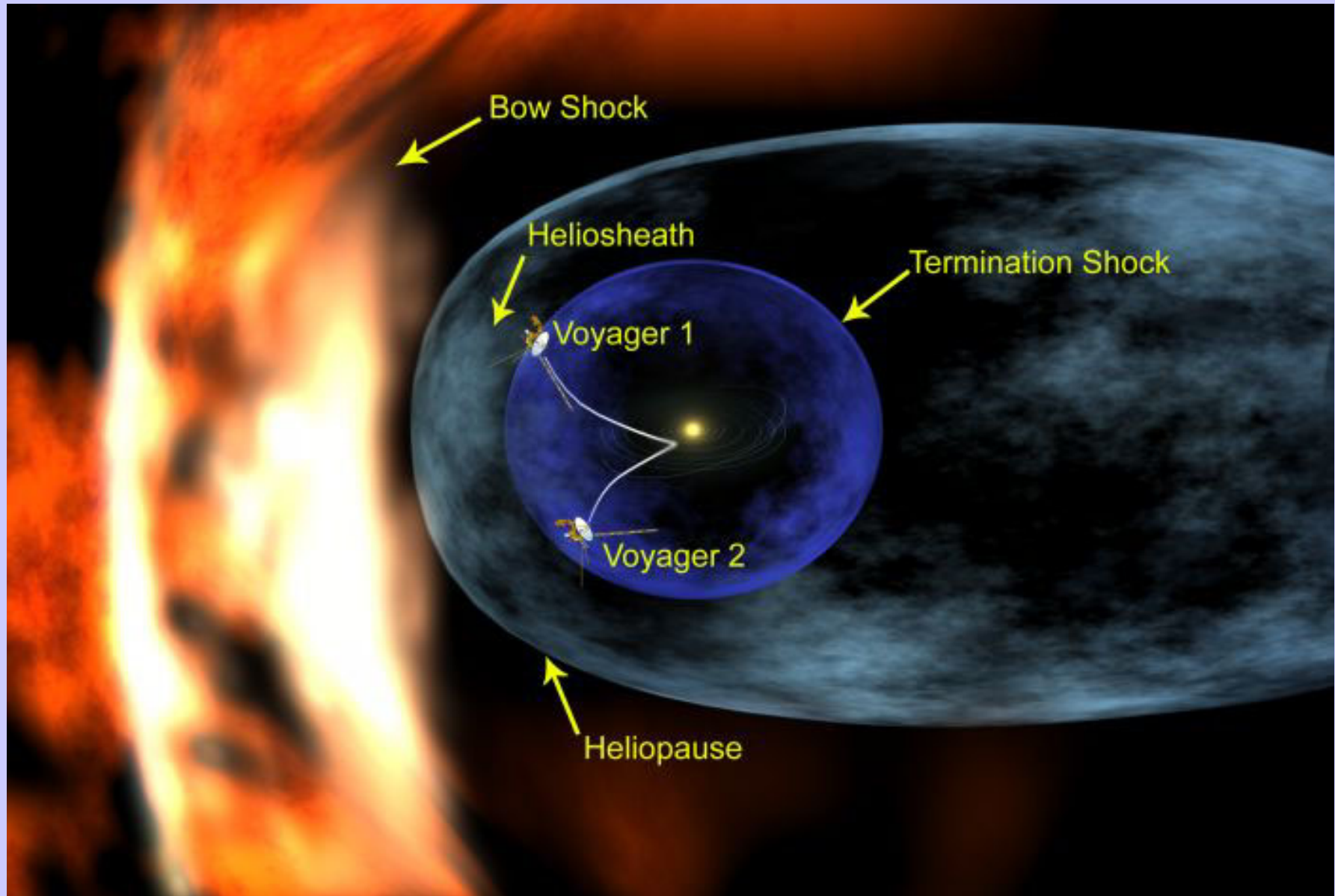
(Blanc, 2004)

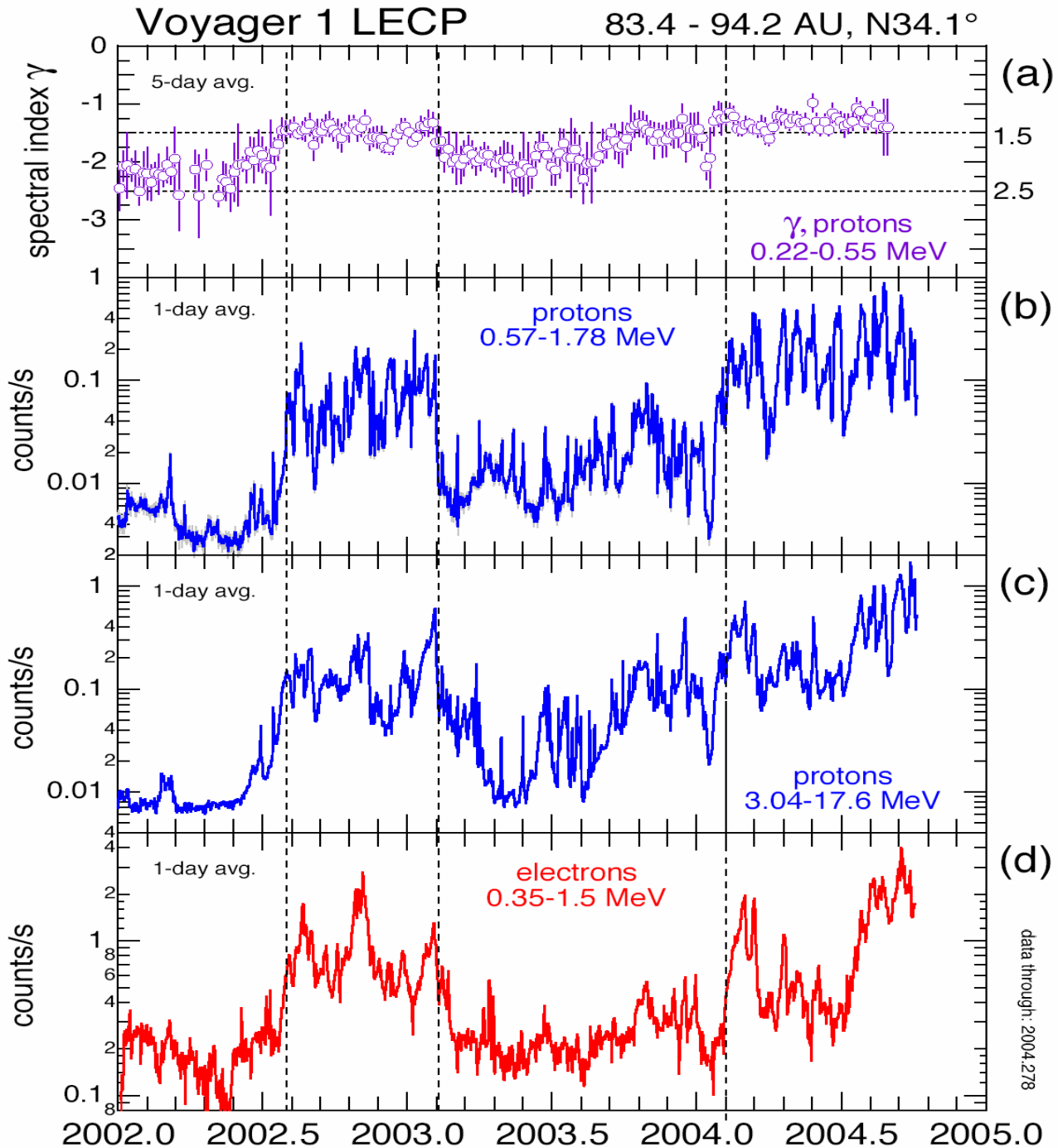


Galactic input:
Plasma, neutrals,
GCR's,
Interstellar dust

Solar system inputs:
Solar wind, neutrals,
SEP's,
Interplanetary dust

Artist's Concept of Heliosphere and Trajectories of Voyagers 1, 2





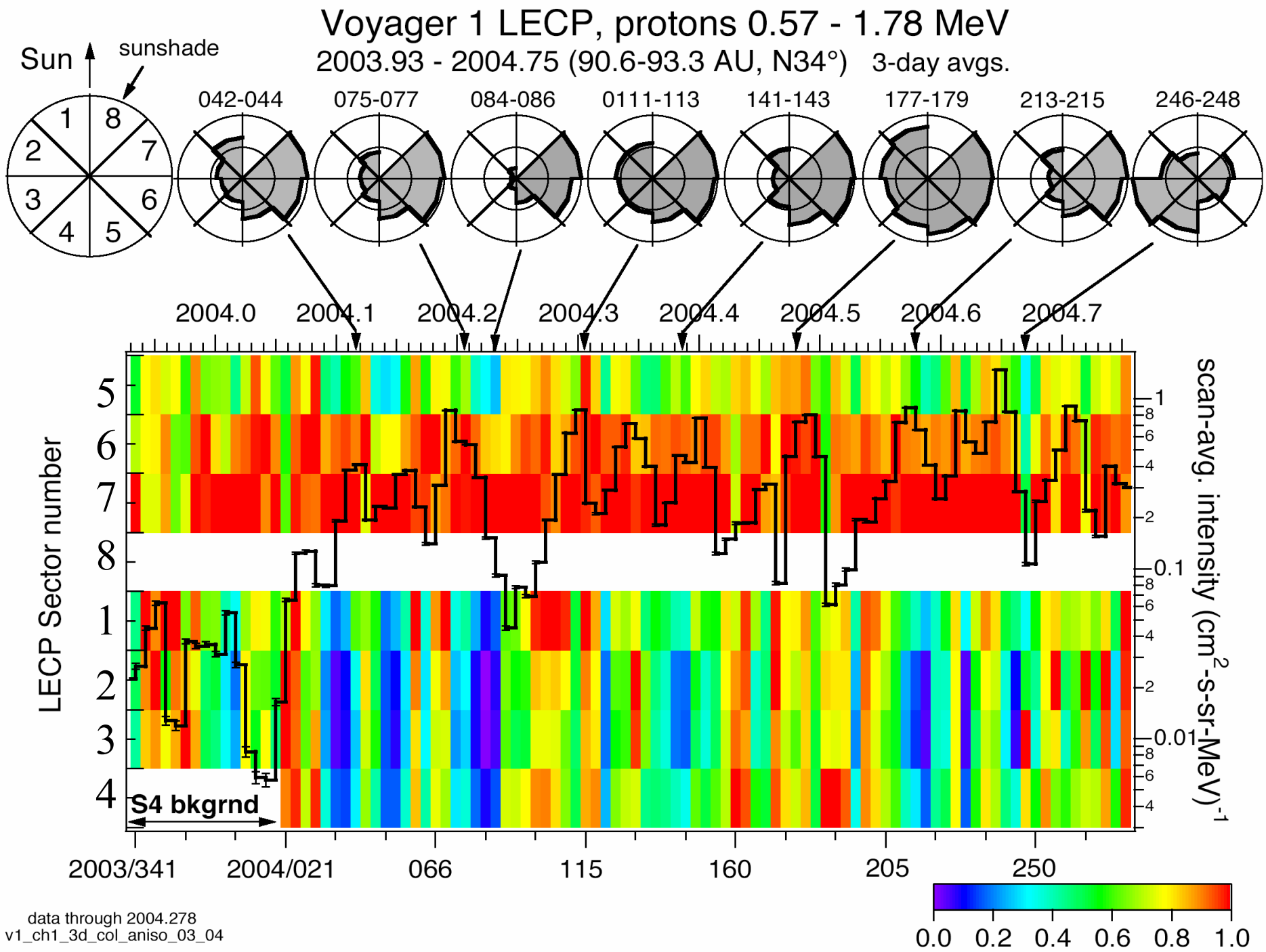
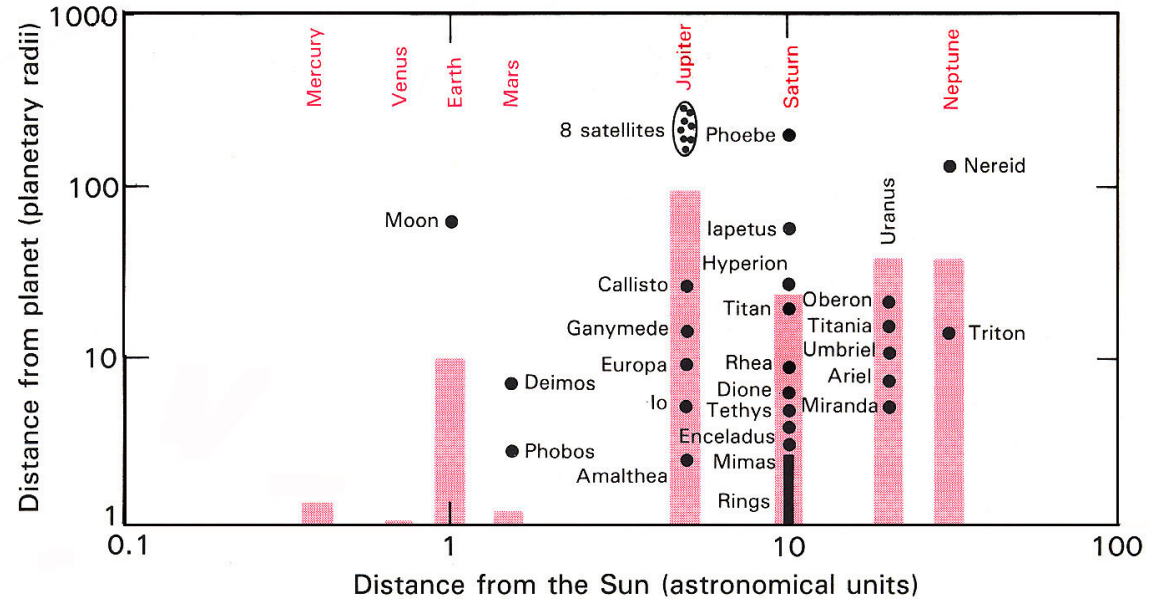


Figure 4—Magnetosphere sizes, satellite locations, and planetary orbital radii. Each vertical bar represents the distance from the center of a planet to the Sunward boundary of its magnetosphere, in units of the planet's radius. The magnetosphere size for Neptune is an estimate. (Adapted from Ref. 5.)



Lanzerotti, L. J. and S. M. Krimigis, Comparative magnetospheres, *Physics Today*, 38, 25-34, 1985.

Van Allen Radiation Belts in the Solar System

- Five planets (Earth, Jupiter, Saturn, Uranus, Neptune) have belts
- One planet may have (transient?) belt (Mercury)--MESSENGER, 2008 is first flyby
- Venus and Mars do not have radiation belts
- Pluto is unlikely to have belt(s)--must wait for New Horizons encounter in 2015!
- Perhaps there is a belt surrounding the Heliosphere at > 85-95 AU

Dr. James A Van Allen

THANK YOU

For the Inspiration, Leadership by example,
Your teaching method, your Trust, and Your friendship
For all your students and colleagues!